Received: 17 July 2021 | Revised: 18 August 2021 | Accepted: 18 August 2021

DOI: 10.1002/jat.4232

RESEARCH ARTICLE

Journal of Applied Toxicology WILEY

Mechanisms and biological impacts of graphene and multi-walled carbon nanotubes on *Drosophila melanogaster*: Oxidative stress, genotoxic damage, phenotypic variations, locomotor behavior, parasitoid resistance, and cellular immune response

Eşref Demir

Vocational School of Health Services, Department of Medical Services and Techniques, Medical Laboratory Techniques Programme, Antalya Bilim University, Antalya, Turkey

Correspondence
Eşref Demir, Vocational School of Health Services, Department of Medical Services and Techniques, Medical Laboratory Techniques Programme, Antalya Bilim University, Antalya 07190, Turkey.
Email: esref.demir@antalya.edu.tr

Funding information
Türkiye Bilimsel ve Teknolojik Araştirma Kurumu, Grant/Award Number: 218Z031

Abstract

The use of graphene and multi-walled carbon nanotubes (MWCNTs) has now become rather common in medical applications as well as several other areas thanks to their useful physicochemical properties. While in vitro testing offers some potential, in vivo research into toxic effects of graphene and MWCNTs could yield much more reliable data. *Drosophila melanogaster* has recently gained significant popularity as a dynamic eukaryotic model in examining toxicity, genotoxicity, and biological effects of exposure to nanomaterials, including oxidative stress, cellular immune response against two strains (NSRef and G486) of parasitoid wasp (*Leptopilina boulardi*), phenotypic variations, and locomotor behavior risks. *D. melanogaster* was used as a model organism in our study to identify the potential risks of exposure to graphene (thickness: 2–18 nm) and MWCNTs in different properties (as pure [OD: 10–20 nm short], modified by amide [NH_2] [OD: 7–13 nm length: 55 μm], and modified by carboxyl [COOH] [OD: 30–50 nm and length: 0.5–2 μm]) at concentrations ranging from 0.1 to 250 μg/ml. Significant effects were observed at two high doses (100 and 250 μg/ml) of graphene or MWCNTs. This is the first study to report findings of cellular immune response against hematopoiesis and parasitoids, nanogenotoxicity, phenotypic variations, and locomotor behavior in *D. melanogaster*.

KEYWORDS
cellular immune response, *Drosophila melanogaster*, *drosophila* parasitoids, genotoxicity, graphene, *Leptopilina boulardi*, locomotor behavior, multi walled carbon nanotubes, phenotypic variations

1 | INTRODUCTION

Over the past decade, nanotechnology has been gaining ground in modern research and engineering, as it allows us to explore and manipulate existing materials on a scale measured in nanometers. It encompasses every technology and science operating on the nanoscale, as well as recently discovered scientific principles and properties during nanoparticles (NPs) research (Demir, 2020b). NPs are described as particles with at least one external dimension measuring 100 nm or below. Common examples of NPs include silver, gold, nickel, copper nanowires, and nanorods, along with silica, metal oxides, carbon nanotubes (single-walled carbon nanotubes [SWCNTs], multi-walled carbon nanotubes [MWCNTs]), and nanocrystals (Dreher, 2004). The physical properties of larger bulk materials do not

usually change depending on their size, whereas at the nanoscale physical and chemical properties of such materials often show remarkable variations—particularly including increased surface-to-volume ratio as the size of material decreases (Sau et al., 2010). For instance, metal oxide nanoparticles (NPs) and CNTs may display larger surface area at smaller sizes, which brings about notable changes in their physicochemical properties and reactivity features (Aillon et al., 2009; Donaldson et al., 2010; Golbamaki et al., 2015). Thanks to such unprecedented characteristics of ultrafine particles that allow a multitude of applications across different sectors including nanomedicine, agriculture, and industry, nanotechnology is now considered "the next big thing" destined to revolutionize the way we tailor materials (Godwin et al., 2015). The production of nanomaterials (NMs) was estimated to surpass 21,713 tons by 2020, and nano-engineered products generated a revenue amounting to $731 billion in 2012 (Lux Research, 2014). Thus, such massive adoption of NMs demands that any potential harmful effects of these materials and their biological interactions be meticulously and extensively examined (Alaraby et al., 2016; Demir, 2020b; Hawkins et al., 2015; Kermanizadeh et al., 2016).

CNTs, on the other hand, have diameters measured in nanometers and lengths in micrometers, which creates almost one-dimensional structures with relatively large length-to-diameter ratio of about 1,000 or below (Aqel et al., 2012; Iijima, 1991). For that reason, they feature unique thermal stability and tensile strength, as well as superior physicochemical, conductive, and mechanical properties (Dresselhaus et al., 2004). These advantages features make CNTs ideal for diverse applications across a number of sectors like electronics, nanomedicine, construction, molecular pharmaceuticals, and targeted delivery of drugs and genes (Asakura et al., 2010; Bianco et al., 2005; Demir, Marcos, 2018b; Hirsch, 2002; Zhang et al., 2014). In contrast, graphene, a two-dimensional high-aspect-ratio material with a single or several double carbon structures arranged in a hexagonal lattice, belongs to a new carbon group NMs (Bianco et al., 2013). Graphene and MWCNTs, thanks to their remarkable physico-chemical properties, have been among the most sought-after materials in medical applications like implants, targeted drug delivery, molecular pharmaceuticals, and cancer treatment, as well as in commercial products including batteries and electrochemical biosensors (Maynard et al., 2006; Sarkar et al., 2018; Shen et al., 2012). Due to this high interest in graphene and MWCNTs, it is imperative that carry out studies to explore adverse effects of these materials.

It was thought that the side effects associated with genotoxicity caused by exposure to graphene and MWCNTs were mainly caused by the effects on the DNA level and the development of carcinogenesis (Guo et al., 2012). However, it is noteworthy that there is a controversy regarding potential genotoxicity because both genotoxic and non-genotoxic effects have been reported (Demir, 2020b; Demir, Marcos, 2018b; Hu & Zhou, 2013; Kermanizadeh et al., 2016; Kumar et al., 2019; Pandey et al., 2019; Priyadarsini et al., 2019; Sood et al., 2019; Zou et al., 2016). The presence of many factors such as characterization, concentration, exposure time, route of exposure, dispersion employed to dissolve nanotubes, and the end-point used in analyses could explain a range of reported effects (Hartmann et al., 2015).

Extensive research is critical to investigate the potential toxicity of NMs by using in vivo models. Serious concerns over high costs and research ethics about animal testing most of the time cause a dilemma among scholars as to the use of standard in vivo tests, or acute toxicity testing in mammals; therefore, more recently researchers opt for simpler experimental models such as roundworms (Chatterjee, Eom, et al., 2014; Chatterjee, Yang, et al., 2014; Contreras et al., 2012; Hunt et al., 2013; Meyer & Williams, 2014), zebrafish (Dedeh et al., 2015; He et al., 2014), and fruit fly species known as *Drosophila melanogaster* (Alaraby et al., 2016). Among these models, *D. melanogaster* stands out as a useful model organism to measure the cytotoxicity and genotoxicity of NMs (Demir, 2020a, 2020b, 2020c). *D. melanogaster* has gained acceptance in research in many biological and medical fields as well as in evolutionary biology, genetics, physiology, ecology, and microbial pathogenesis. It is estimated that about 60% of *D. melanogaster* DNA is the same as humans, and approximately 75% of our genetic material associated with several human diseases like cancer, autism, and diabetes has functional homology in the fruit fly (Lloyd & Taylor, 2010). In addition, *D. melanogaster* is a model organism that enables research on the mechanisms that cause immunity, aging and oxidative stress, Alzheimer's disease (Latouche et al., 2007), spinocerebellar ataxia, or SCA (Latouche et al., 2007), and neurodegenerative disorders (Bier, 2005). Another important feature of *D. melanogaster* is that it has certain molecular pathways and biological mechanisms shared with higher mammals (U.B. Pandey & Nichols, 2011; Wang et al., 2012), making it insect an ideal testing model for numerous fields including genotoxicity studies (Pandey & Nichols, 2011), pharmacology (Pandey & Nichols, 2011), and neurotoxicity testing of many chemicals (Rand, 2010). More importantly, *D. melanogaster* allows researchers to avoid serious ethical barriers set against the use of vertebrates or larger mammals in animal experiments (Jennings, 2011). Considering all these advantages, researchers have been increasingly employing *D. melanogaster* for evaluating the toxicity of NMs. For this reason, many studies have been used as such an experimental organism to evaluate cytotoxicity, genotoxicity, generation of reactive oxygen species (ROS), morphological deformations, pigmentation color, and changes in gene expression that occur after exposure to various NMs. Furthermore, *D. melanogaster* is the primary model organism commonly used in the field of insect immunology and genetics to explore the underlying mechanisms of insect immune response (Leitão et al., 2019). The interaction between parasitoid wasps and *D. melanogaster* is a model system for both evolutionary biologists and immunologists. Insect immunology provides vital information on the potential for transmission of disease vectors that carry fatal diseases such as malaria. Parasitoid wasps alone may represent up to 20% of all insect species worldwide and include the common fruit fly *D. melanogaster* infecting parasitoids *Leptopilina boulardi*, *Leptopilina heterotoma*, and *Asobara tabida* (Lasalle & Gauld, 1991). Parasitoid wasps, such as *L. boulardi*, are a

naturally occurring threat to many insect species including the common fruit fly *D. melanogaster* in ecological systems. A parasitoid wasp infection commences with the deposition of a wasp egg into the larvae of host species, after which the fly/wasp arms race for survival commences. One of three possible outcomes can occur: (1) host immune suppression and wasp survival, (2) encapsulation of the wasp egg and host survival, or (3) both organisms die (Godfray, 1994; Nappi, 1975).

Continuous or acute exposure to NMs might trigger a variety of immune reactions in humans because they are foreign bodies to our immune system; for that reason, research into NM-immune interaction is of vital importance, as urgently need to gain better insight into such interactions to deal with safety concerns of NMs. A thorough characterization of physical and chemical properties of NMs is considered a prerequisite for research on their immune-nanogenotoxicity. In this regard, comprehensive immune-genotoxicity studies are warranted to determine the risks of NM exposure associated with human diseases (Ng et al., 2019).

The innate immune system of *Drosophila* could serve as an ideal model in collecting valuable information about the innate immune system of humans and other mammals, especially through a series of experiments on larval hemocytes (Hiroyasu et al., 2018; Zettervall et al., 2004). In the current literature, there exist some research reporting findings on genotoxic properties of graphene or MWCNTs; however, to our knowledge, no study has been conducted to explore parasitoid resistance and cellular immune response against two different lines (NSRef and G486) of parasitoid wasp (*L. boulardi*) related with graphene or MWCNTs on *D. melanogaster*. Hence, this study was carried out to identify and characterize egg-to-adult viability (toxicity), morphological deformations, locomotor behavior, phenotypic variations in different generations, genotoxic effects (primary and oxidative DNA damage in hemocytes and somatic mutations or recombinations in the fly's wing imaginal disc cells), intracellular ROS production by hemocytes of *Drosophila* larvae, parasitoid resistance, and cellular immune response upon exposing *D. melanogaster* larval hemocytes to graphene or MWCNTs.

2 | MATERIALS AND METHODS

2.1 | Chemicals

Graphene nanoplatelets (purity: >95%, graphene thickness: 2–18 nm with less than 32 layers, CAS no. 7782-42-5), short multi-walled carbon nanotubes (MWCNTs) (purity: >95%, OD: 10–20 nm, CAS no. 99685–96-8, length: 10–30 μm), MWCNTs (amide [NH_2] functionalized, purity: 95%, OD: 7–13 nm, length: 55 μm]) and MWCNTs (carboxyl [COOH] functionalized, purity: >90%, OD: 30–50 nm, length: 0.5–2 μm, CAS no. 99685-96-8) were purchased from US Research Nanomaterials, Inc. (Houston, TX, USA). The rest of the chemicals used in the study were purchased from Sigma Chemical Co. (St. Louis, MO). Prior to use, graphene or MWCNTs were dispersed in 1% isopropanol (IPA).

2.2 | Characterization and dispersion of graphene and MWCNTs

A series of analyses involving transmission electron microscopy (TEM), dynamic light scattering (DLS), and laser Doppler velocimetry (LDV) were carried out to characterize graphene or MWCNTs (as pure, NH2 functionalized and COOH functionalized). TEM microscopy technique was performed by Tecnai G2 F30 (Austin, Texas, USA) and FEI, QUANTA 260 F (Hillsboro, Oregon, USA) to determine size and morphology of NMs. The DLS and LDV studies were conducted with Malvern Zetasizer Nano-ZS zen3600 (Worcestershire, UK) to identify their hydrodynamic size and zeta potential. Prior to dispersion, pre-wetting procedure was applied to graphene or MWCNTs in 0.5% absolute ethanol, and then, the NMs were dispersed in 0.05% bovine serum albumin (BSA) in MilliQ water to enhance the workability. The graphene or MWCNTs in the dispersion medium were subjected to ultrasonic vibration at 20 kHz for 30 min by means of Branson Digital Sonifier system (S-250D) (Danbury, Connecticut, USA) to create a stock dispersion of 2.56 mg/ml, in accordance with the Nanogenotox protocol (Jacobsen et al., 2010; Nanogenotox, 2011).

2.3 | Endotoxin assay for graphene and MWCNTs

In order to check endotoxin contamination in NMs, the endotoxin content was quantified through chromogenic Limulus amebocyte lysate (LAL) assay (Lonza [QCL-1000TM], Inc., Walkersville, MD) (www.lonza.com/qcl1000), in accordance with the protocol specified in the manual, as well as in previous research (Lankoff et al., 2013; Demir, Marcos, 2018a, 2018b; Demir et al., 2020). All test tubes were rendered free of pyrogenic material by heating at 200°C. Subsequently, the standard amount (50 ml) of test sample was added to the test wells, and then, it was heated in the 96-well plates at 37°C. For each sample, a minimum of three wells were used. The linearity of the standard was confirmed by lipopolysaccharide (LPS). A standard curve (ranging from 0.1 to 1 EU/ml) was created over the concentration range 0.117667–0.998 EU/ml and compared to the reference range (*Escherichia coli* E50-640) for each assay. For endotoxin testing, endotoxin standards and dilutions of samples were assessed in pyrogen-free microplates (Costar No. 3596; Corning, Inc., Corning, NY) in a BioTek Synergy 2 microplate reader (BioTek, Winooski, VT) at 37°C. Absorbance was performed at 405–410 nm. Commercially available control endotoxins (lipopolysaccharide, LPS; 0.5 EU/ml) and LAL water as positive and negative controls were used as standards. To determine the spike recovery, the percentage of recovery spike values was calculated as follows:

$$\text{Recovery spike value}\,(\%) = \frac{a-b}{c} \times 100.$$

In this formula, *a* represents the amount of endotoxin found in spiked sample, while *b* stands for the amount of endotoxin found in the sample, and *c* represents the amount of added endotoxin.

The calculated recovery spike values were 98.4%, 100%, 100%, and 123.8% for graphene (0.1, 10, 100, and 250 μg/ml); 102%, 101.2%, 101%, and 103.2% for MWCNTs-pure (0.1, 10, 100, and 250 μg/ml); 41.8%, 113.4%, 188.8%, and 188.4% for MWCNTs-NH_2 (0.1, 10, 100, and 250 μg/ml); and 40.4%, 125.8%, 187.8%, and 188% for MWCNTs-COOH (0.1, 10, 100, and 250 μg/ml), respectively.

2.4 | *D. melanogaster* strains, exposure, toxicity, and morphological alterations

The *Drosophila* larvae and adults at 25 ± 1°C and at a humidity level of 60% on food media consisting of cornmeal, sugar, yeast, agar, propionic acid, and Nipagin were cultured. A total of three different mutant fruit fly strains in the study: wild Canton-S, *flare-3*, and multiple wing hairs strains were included. In the wing SMART (somatic mutation and recombination test), two distinct fly strains: *flare-3* with genetic constitution *flr*^{3}/*In* (*3LR*) *TM3*, *Bd*^{s}, and multiple wing hairs with *mwh/mwh* genetic constitution were used. Further data as to the descriptions and genetic markers of mentioned phenotypes were previously published by Lindsley and Zimm (1992). As for other experiments, only the wild Canton-S strain was utilized in testing. To investigate toxic potential of graphene or MWCNTs were measured and recorded egg-to-adult survival rates in flies. The adult flies of Canton-S strain were placed in bottles containing food medium, specifically darkened with an addition of carbon powder in a manner that would allow easy collection of fly eggs every 8 h. After that, each test sample consisting of 50 fly eggs was transferred to plastic vials that contained 4 g of instant food medium designed for *Drosophila* (Carolina Biological Supply Co., Burlington, NC). The medium was previously saturated with 10 ml of different concentrations of graphene or MWCNTs (0, 0.1, 10, 100, and 250 μg/ml) dispersions, and the final concentrations of food media for NMs were 0.0002, 0.0022, 0.0222, and 0.0556 mg/g. The concentrations are indicated as μg/ml for in the text. These concentrations were selected according to previous literature values for *Drosophila* (de Andrade et al., 2014; Demir, Marcos, 2018b; Kumar et al., 2019; Leeuw et al., 2007; Liu et al., 2009; Liu et al., 2014; Machado et al., 2013; Pandey et al., 2019; Philbrook et al., 2011; Priyadarsini et al., 2019; Siddique et al., 2013; Siddique et al., 2014; Sood et al., 2019; Vega-Alvarez et al., 2014; Zou et al., 2016).

The ideal dose of ethyl methanesulfonate (EMS) concentration (1 mM) that would produce effective mutagenesis was determined based on the evidence from our previous work (E. Demir, Marcos, 2018a). Preliminary tests to confirm the toxic potential of the NMs. The various concentrations of graphene or MWCNTs (as pure, COOH functionalized, and NH_2 functionalized) were determined in such a manner that the highest dose would not exceed 250 μg/ml. A total of five different replicate samples per concentration were used. The adult flies surviving after the exposure were finally collected and counted for the calculation of survival rate as compared to controls.

In an attempt to find out whether exposure to graphene or MWCNTs during egg-to-larvae phase caused any developmental changes in the surviving adult flies, 100 adult flies per treatment were thoroughly examined through stereomicroscopy (SLX-2 STEROEZOOM). The detected morphological changes in different body parts, including the head, thorax, legs, wings, and abdominal area, were carefully recorded.

While *mwh* single spots detected in the wing spot assay could be caused by somatic DNA recombination, substitution, or deleted wild-type alleles, the *flr*^{3} single spots usually occur as a result of small deletion of wild-type alleles. Wing blade twin spots comprising both *mwh* and *flr*^{3} subclones have been found to originate entirely from recombination during mitosis between the centromere and the *flr*^{3} locus (Graf et al., 1984). Carefully examined 80 fly wings from 40 individuals in each doses. Standard procedures previously described for the wing-spot test for *Drosophila* were followed during the scoring of flies and data analysis, in a parallel manner employed in most recent studies (Demir et al., 2015; Demir, Marcos, 2018a).

The rate of the recombinogenic effects on the flies was calculated as follows, as per Demir et al. (2014):

$$\text{Recombination}\,(\%) = \frac{a-b}{c} \times 100.$$

In this formula, *a* represents frequency of total *mwh* spots in marker heterozygous wings (*mwh/flr*^{3}), and *b* represents frequency of total *mwh* spots in balancer heterozygous wings (*mwh/TM3*) induced by exposure to graphene or MWCNTs (250 μg/ml).

2.5 | Intracellular oxidative stress (ROS) detection

Intracellular levels of ROS were measured by 2′,7′-dichlorodihydrofluorescein diacetate (DCFH-DA) assay in hemocytes collected from *Drosophila* larvae following their exposure to graphene or MWCNTs (Demir & Marcos, 2017). Our previously published protocol was followed (Demir, 2020c; Demir & Marcos, 2017, 2018a). Briefly, hemocytes were collected and exposed to 5 mM DCFH-DA for 30 min at 24°C. The fluorescence of the cells was quantified using a fluorescent microscope with an excitation of 485 nm and an emission of 530 nm (green filter). Hydrogen peroxide (H_2O_2, 0.5 mM) was used as a positive control. ImageJ program was used for the quantitative evaluation of fluorescent images from both control and treated larvae.

2.6 | Comet assay

The Comet assay to detect induction of DNA breakage was used. *Drosophila* larvae hemocytes were used as target cells. The procedures previously laid out in the literature were strictly followed during the Comet assay (Demir & Marcos, 2017, 2018a; Singh et al., 1988). Third-instar larvae (72 ± 4 h old) were transferred into plastic vials containing 4 g of *Drosophila* instant medium (Carolina Biological Supply Company, Burlington, NC), pre-wetted with the following concentrations: control (distilled water) at 0, study groups at 0.1, 10, 100,

and 250 μg/ml of graphene or MWCNTs for 24 ± 2 h. Clean distilled water was used as a negative control (Demir et al., 2013), while EMS (4 mM) (Demir & Marcos, 2017) was used as positive control.

2.7 | Phenotypic variations

The F0 (parent), F1, F2, and F3 generation flies of control and graphene or MWCNTs exposed were carefully observed under stereo microscope (SLX-2 STEROEZOOM) for the phenotypic variations in head, eye, mouth, thorax, legs, wings, and abdominal area. Published protocols in the literature were followed (Anand et al., 2017; Priyadarsini et al., 2019). One-thousand five-hundred randomly selected flies (500 flies on each one of the three replicate) were analyzed for each concentration of graphene or MWCNTs in a particular generation.

2.8 | Climbing assay

In an attempt to examine the flies' locomotor ability, a climbing assay was performed by following the procedures laid out by Pendleton et al. (2002) and Anand et al. (2017). Accordingly, 10 fruit flies from both control and study groups exposed to graphene and MWCNT groups were separately transferred to vials, where they were acclimatized for 15 minutes at room temperature. The vials were gently tapped to send the flies down to the bottom and then measured for their climbing ability; the number of flies managing to climb above the 7 cm mark within 10 s in each group was recorded. This climbing ability assay was repeated 10 times for the same group after each treatment.

2.9 | Wasp maintenance

Stocks of wasps were maintained on cornmeal food (per 1,200 ml water: 13 g agar, 105 g dextrose, 105 g maize, 23 g yeast, 35 ml Nipagin 10% w/v). The insects were kept at 25°C in a 14-h light and 10-h dark cycle at a humidity level of 70%. Two *Leptopilina boulardi* strains were used: G486 strain (Dupas et al., 1998) known for low virulence and NSRef (Varaldi et al., 2006) high virulence. A vulnerable outbred stock of *D. melanogaster* was utilized to maintain the two wasp strains by following the protocol previously laid out in the literature (A.B. Leitão et al., 2019).

2.10 | Parasitoid resistance (encapsulation assay)

Adult flies laid eggs on agar plates during the night (between 6 pm and 9 am). The eggs were transferred into microcentrifuge tubes (volume 1.5 ml) in 500 μl PBS, and 15 μl of them in PBS (~150 eggs) was then transferred to cornmeal food plates (50 mm diameter) to continue maintenance at 25°C for 48 h. During this phase, the flies were aged between 48 and 63 h, so all strains were in late first or early second instar stage. Second-instar *Drosophila* larvae were transferred into culture vials (40 larvae per vial), and three female wasps were added into each vial, and then, the wasps were removed from vials 3 h later. The vials containing the larvae were incubated for 12 days (adult formation) and when flies emerged, they were squashed between two glass slides to assess the encapsulation, which was calculated as the number of flies with capsules divided by the total number of infected larvae in each of the vials. To measure the rate of encapsulation in larvae, the *Drosophila* larvae were dissected in PBS 48 h after infection, and the presence of encapsulated wasp eggs or larvae was determined.

The formula used to calculate encapsulation rate (ER) is detailed below (Martinez et al., 2012; McGonigle et al., 2017):

$$ER = \frac{A}{B - C}.$$

In this formula, *A* represents the average number of flies in the vials infected by the parasitoid wasps as scored based on the presence of a melanized capsule, while *B* represents the average number of flies in control vials, and *C* represents the mean number of flies in treatment vials which were not infected by the parasitoid wasps.

The formula used to calculate encapsulation rate is detailed below (Martinez et al., 2012; McGonigle et al., 2017):

$$\text{Encapsulation rate} = \frac{\text{Number of observed capsules}}{\text{100-Number of infected live flies}}.$$

2.11 | Hemocyte counts

Adult *Drosophila* flies were left on agar plates to lay eggs overnight (between 6 pm and 9 am). The eggs were transferred into microcentrifuge tubes (volume 1.5 ml) in 500 μl PBS, and 15 μl of them in PBS (~150 eggs) was then transferred to cornmeal food plates (50 mm diameter) to continue maintenance at 25°C for 48 h. During this phase, the flies were aged between 48 and 63 h, so all strains were in late first or early second instar stage. Three female wasps were added into treatment vials, whereas the controls were prepared under the same conditions without infection. About 48 h after the infection, the larvae were removed from food medium with 15% w/v sugar solution. They were washed with ultrapure H_2O and then dried on some filter paper. Stocks of 10 to 12 larvae were transferred into a porcelain dissection dish, and they were incised to let them bleed from the ventral side; 1 μl of hemolymph was removed and diluted in 9 μl of neutral red (1.65 g/L PBS). About 10 μl of hemolymph dilution was put into a Thoma counting chamber, and hemocytes were counted in an area of 1 mm^2, accounting for a volume of 0.1 μl. Plasmatocytes and lamellocytes were then categorized according to their size and shape. Fiji program was employed to quantify both control and treated larvae on fluorescent images using a fluorescence

microscope (Olympus BX50) equipped with a 480–550 nm wide-band excitation filter and a 590 nm barrier filter (Schindelin et al., 2012). The induction rate of the number of hemocytes was calculated by using the method specified by Abraham (1994):

$$\text{Induction}\,(\%) = \frac{a-b}{a} \times 100.$$

In this formula, *a* represents the number of hemocytes induced by graphene or MWCNTs alone, and *b* represents the number of hemocytes induced by graphene or MWCNTs in the presence of *L. boulardi* infection (NSRef or G486).

2.12 | Statistical analysis

The differences between the frequencies of each type of spot in treatments and the concurrent negative controls were assessed by the conditional binomial test of Kastenbaum and Bowman (1970) on the MICROSTA program, with significance levels of $\alpha = \beta = 0.05$. The multiple decision method developed by Frei and Würgler (1988) was utilized to classify overall responses as positive, weakly positive, negative, or inconclusive. Research data were also analyzed by the Mann–Whitney–Wilcoxon non-parametric *U* test to exclude false positive and negative results (Frei & Würgler, 1988, 1995), and a *P* value equaling or less than 0.05 ($P = 0.05$) was considered significant.

The normality of variance was analyzed by Kolmogorov–Smirnov and Shapiro–Wilk test, and homogeneity of variance was evaluated by Levene's test. Data that followed normal distribution and equal variance (Comet assay and the endotoxin assay) were analyzed with the Student's *t* test, using SigmaPlot version 11.0 (SPSS, Chicago, IL). The data following normal distribution and equal variance (climbing assay) were further analyzed by one-way ANOVA on SigmaPlot version 11.0 (SPSS, Chicago, IL). Data with unequal variance or skewed distribution (viability, ROS production, and hemocyte counts) were assessed by the non-parametric Mann–Whitney *U* test. Findings were considered statistically significant when the *P* value was ≤0.05. All data from experiments are presented as means of two independent experiments, including duplicates of each one of these, unless stated otherwise. The values of the parameters were calculated and presented as arithmetic mean ± standard error.

3 | RESULTS

3.1 | Characterization of graphene and MWCNTs

The NMs used in the study were characterized by using different techniques including TEM, SEM, EDX, DLS, and LDV. Results are presented as supporting information (Figures S1–S4). Examples of TEM and SEM figures are shown in Figures S1A,B, S2A,B, S3A,B, and S4A, B. The average diameters obtained using DLS were 116.90 ± 2.25 nm, 178.40 ± 3.68 nm, 172.80 ± 2.73 nm, and 170.80 ± 3.42 nm for graphene or MWCNTs, respectively (Figures S1D, S2D, S3D, and S4D). Polydispersity Index (PDI) obtained using DLS were 0.289 for graphene and 0.447, 0.409, and 0.414 for MWCNTs, respectively. Zeta potential average calculated by the LDV technique was 15.80 ± 2.687 mV, −9.86 ± 2.317 mV, −2.83 ± 1.935 mV, and −7.80 ± 1.04 mV for graphene and MWCNTs, respectively (Figures S1D, S2D, S3D, and S4D). Relatively high values of hydrodynamic diameter and relatively lower zeta potential values suggest tendency of NMs to aggregate. In order to avoid more aggregation, all experiments were carried out by utilizing freshly sonicated NM dispersions. The carbon peaks detected by TEM in energy dispersive X-rays microanalysis (EDX) were 95.12%, 95.39%, 97.34%, and 90.9% (Figures S1C, S2C, S3C, and S4C). On the other hand, peak carbon values in energy dispersive X-rays microanalysis (EDX) conducted by SEM were 97.67%, 86.42%, 90.82%, and 83.85% (Figures S1C, S2C, S3C, and S4C).

3.2 | The endotoxin level of NMs

The endotoxin levels of NMs used in this study were measured through the LAL assay (Figure S5). Endotoxin levels at all different concentrations were below the reference limit of detection (0.117667 EU/ml). The detected levels of endotoxins at the greatest concentration (250 μg/ml) were 0.025, 0.036, 0.037, and 0.038 EU/ml, which meant that none of the NMs were contaminated with endotoxins.

3.3 | Toxicity of graphene and MWCNTs

Prior to any testing, the toxicity of the solvent (IPA) was assessed in the study. The results showed that it had a viability (egg to adult survival in *Drosophila*) of 96% for a concentration of 1% of IPA. The viability of clear distilled water was 100%. The toxic effects of the exposure to graphene or MWCNTs, applied during the entire larval development, were specified as variations in the ability to reach the adult stage. Detrimental toxic effects of NMs were observed at doses higher than 250 μg/ml (i.e. 500, 750, and 1,000 μg/ml). Upon exposure to 250 μg/ml of graphene or MWCNT, about 75%, 73%, 71%, and 70% of the treated eggs managed to reach adult stage, respectively. Based on these observations, graphene or MWCNTs (250 μg/ml) may be considered as nontoxic chemicals in *D. melanogaster*. The highest toxicity of MWCNTs-NH_2 was observed at the highest doses, with viability levels of 20%, 17%, and 11% following exposure to NMs at 500, 750, and 1,000 μg/ml, respectively (Figure 1).

3.4 | Reactive oxygen species (ROS) in hemocytes

ROS inhibition in hemocytes of third-instar larvae was examined after exposure to graphene or MWCNTs, and compared to untreated

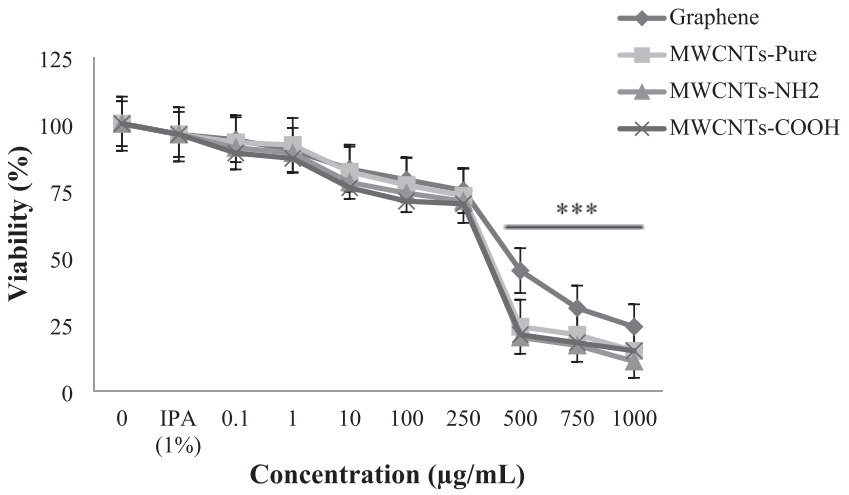

FIGURE 1 Toxicity of graphene or MWCNTs (as pure, amide [NH_2] functionalized and carboxyl [COOH] functionalized) in *D. melanogaster*. Toxic effects were measured as loss of viability (egg to adult survival) related to the control values. $N = 5$ vials per concentration, with 50 eggs/vial. The statistical approach was analyzed with the Mann–Whitney *U* test. $^{***}P \leq 0.001$ compared to control

controls (Figure 2A–E). The potential presence of graphene or MWCNTs in the hemolymph presumes that these materials might interact with hemocytes producing biological effects. The results indicated that graphene or MWCNTs exposure induced higher dose-dependent ROS production in hemocytes, reaching significance at the highest tested doses (100 and 250 µg/ml). The concentrations of 100 and 250 µg/ml have statistically significant for oxidative stress. ROS values in the highest concentration (250 µg/ml) were higher in MWCNTs-NH_2 (290%) than in graphene or MWCNTs (as pure and COOH functionalized) (275%, 281%, and 284%, respectively), suggesting that MWCNTs-NH_2 exhibited greater oxidative stress than other NMs (Figure 2E).

3.5 | Genotoxicity studies

3.5.1 | The comet assay

The Comet assay for hemocytes exposed to NMs showed significant dose-dependent increases in the rate of DNA-strand breaks as compared to negative controls (IPA, 1%). To confirm that no special toxicity was induced in hemocytes due to the larval treatments or by the isolation procedure, previously, a viability assay was conducted. This was carried out using the Trypan blue viability approach. As indicated, no significant toxicity effects were observed for neither of graphene used or for the MWCNTs (data not shown). In addition, Comet assay findings noted that NMs failed to markedly affect levels of DNA damage in hemocytes from the *Drosophila* larvae (Figure 3A). The greatest DNA damage was detected at doses of 100 and 250 µg/ml, which suggests that MWCNTs-NH_2 could be more genotoxic than the others. The relative genotoxic potencies according to the observed DNA damage at the highest concentration (250 µg/ml) are as follows: MWCNTs-NH_2 (40.22% of DNA tail), graphene (38.26% of DNA tail), MWCNTs-COOH (36.54% of DNA tail), and MWCNTs-Pure (34.71% of DNA tail) (Figure 3A). Evidence indicates tail length may be associated with adverse effects.

The results show positive values for that significant increases on oxidative DNA damage values were observed at highest concentration of NMs (250 µg/ml). The net oxidative damage was calculated by subtracting the baseline DNA damage level from the value obtained from the corresponding enzyme. The values were observed with Endo III enzyme were higher than those obtained using Fpg, though they failed to reach a significant level. Therefore, oxidation at purine bases detected by Fpg could be suggested to exert no important genotoxic effect after exposure to graphene or MWCNTs. These effects were observed in all NMs (Figure 3B), and such effects were evaluated as the percentage of DNA in fly tail as a measure of genotoxicity.

3.5.2 | The wing-spot assay

Tables 1–4 show the results found in transheterozygous larvae and balancer heterozygous larvae exposed to various doses of graphene or MWCNTs. These NMs were administered to third-instar larvae at doses ranging from 0.1 to 250 µg/ml. The larvae were constantly exposed to such doses throughout the period lasting until the completion of larval development. Single mutant spots are known to be caused by somatic mutations or somatic DNA recombination, and twin spots are known to appear only as a result of somatic mutations. The results indicated that graphene or MWCNTs (250 µg/ml) induced significant increases in the incidence of small *mwh* single spots, large single spots, in the total number of *mwh* spots, and in the total number of mutant spots, depending on the dose to which flies were exposed. The presence of small or large spots is not considered to be determined by the genotoxic potency of an agent; instead, it is determined by on the length of time during which it reaches the target cells. That points to the fact that these NMs progressed through the wing imaginal disks rather slowly and only caused DNA damage at final stages of development. Significant increases were observed in the positive control of each type of mutant clone upon treatment with EMS (1 mM). The results indicated high level of mutagenic and recombinogenic effects of EMS (Graf et al., 1984).

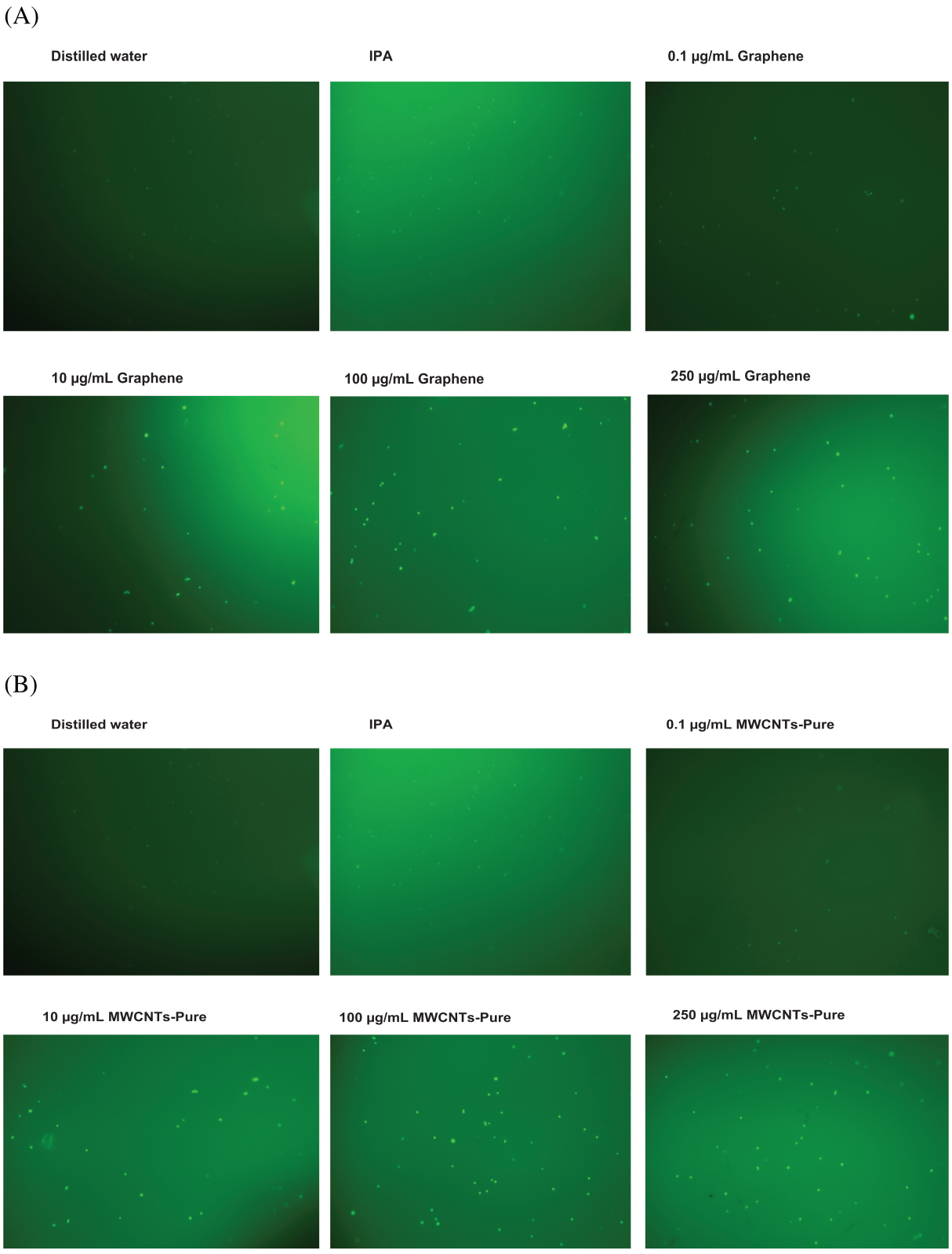

FIGURE 2 ROS production in hemocytes of third instar of untreated (0) and treated larvae exposed to different concentrations (0.1, 10, 100, and 250 µg/ml) of graphene or MWCNTs (as pure, amide [NH_2] functionalized and carboxyl [COOH] functionalized) (A–D). Hemocytes were incubated with 5 µM DCFH-DA at 24°C for 30 min and observed using fluorescent microscopy. The fluorescence intensity of the hemocytes of treated larvae with graphene or MWCNTs were quantified by ImageJ analysis (E); 0.5 mM H_2O_2 was used as positive control. $^{***}P \leq 0.001$ when compared to the negative control using Mann–Whitney *U* test

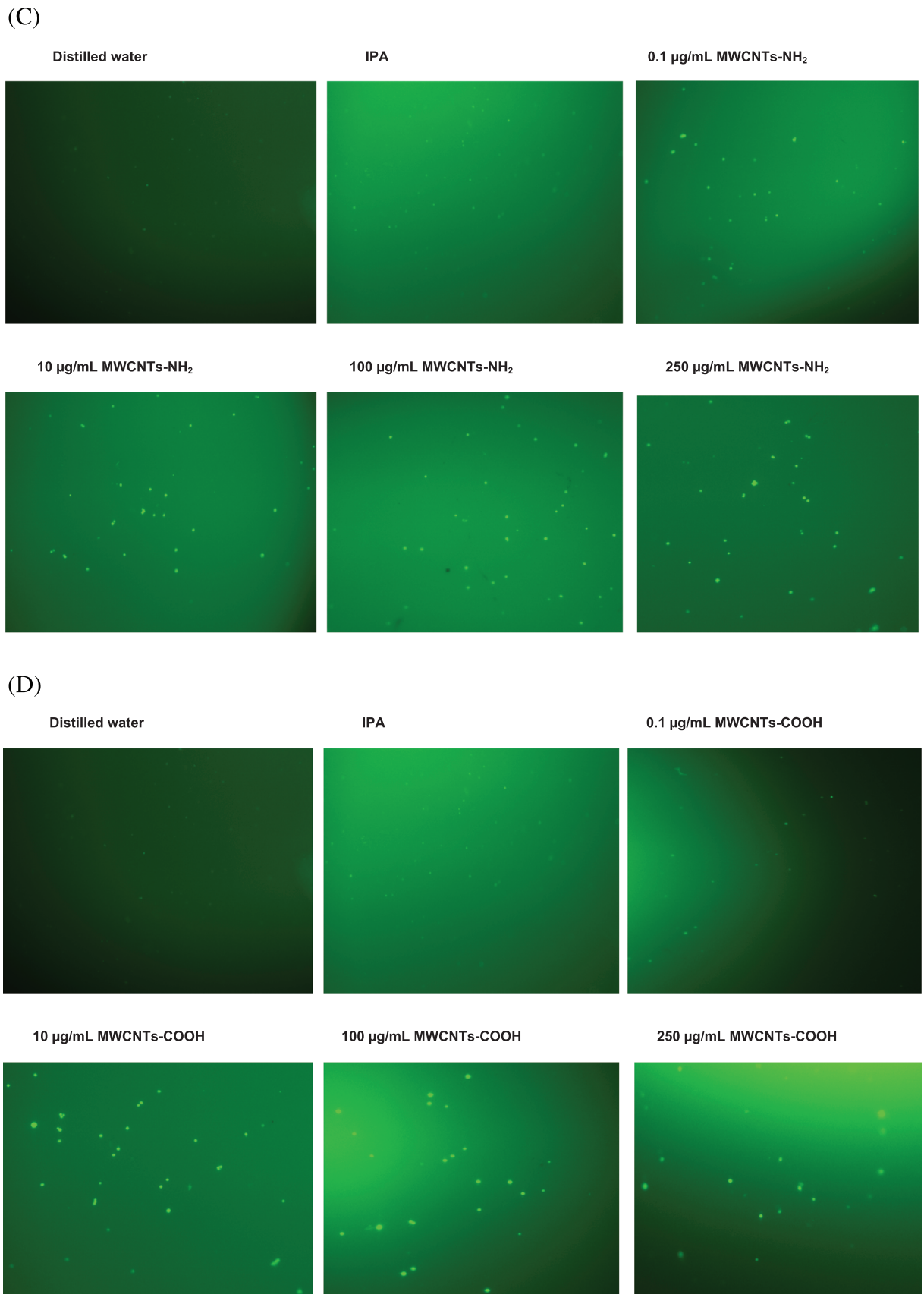

FIGURE 2 (Continued)

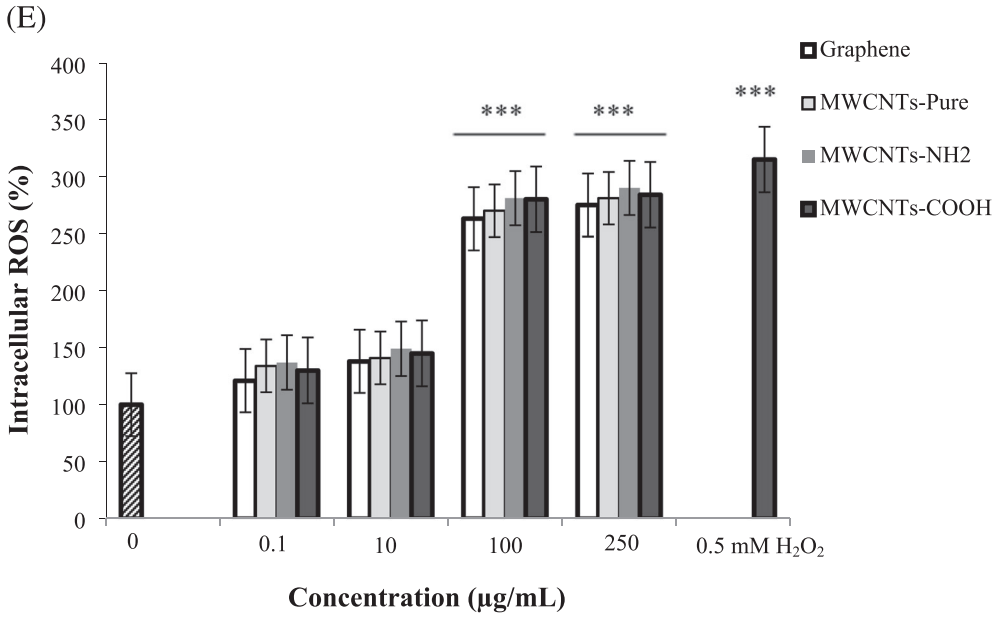

FIGURE 2 (Continued)

In an attempt to have a better understanding of mechanisms by which graphene or MWCNTs (250 µg/ml) induced mutant spots, carried out another experiment with balanced heterozygous larvae. Somatic gene recombination is often suppressed in this genotype, and only clones initiated by somatic mutations are monitored; however, no significant single or total mutant clones could be observed. The results of this experiment are summarized in Tables 1–4. These findings suggest that exposure to graphene or MWCNTs may lead to genotoxicity mainly via somatic DNA recombination route. Despite the lack of statistically significant detrimental impacts, should note that the NM-exposure led to a concentration-dependent rise in the rate of mutant clones.

The fraction of mutants in transheterozygous flies due to recombination increased from 40% to 75.76% upon exposure to the largest dose (250 µg/ml) of graphene or MWCNTs (Tables 1–4). The greatest recombinogenic effect was observed after exposure to 250 µg/ml MWCNTs-NH_2 (75.76%). This was followed by graphene exposure at 250 µg/ml (66.67%), MWCNTs-COOH exposure at 250 µg/ml (42.86%) and MWCNTs-Pure exposure at 250 µg/ml (66.67%) in a descending order (40%).

3.6 | Morphological alterations

In addition to egg-to-adult survival rates examinations, also the possible effects of the NMs that occurred during metamorphoses were examined. It should however note that *Drosophila* flies develop into adults inside the pupae, so they are exposed to compounds from the larval imaginal disks throughout the complete larval development. A thorough morphological analysis of various structures found in adult flies, such as eye, mouth, abdomen, legs, and wings revealed that morphological alterations occurred upon exposure to graphene or MWCNTs. The morphological defects observed in two highest concentrations (100 and 250 µg/ml) of NMs. Figure 4A represents normal phenotypes of adult *D. melanogaster*. A morphological defect in the eye (Figure 4B), mouth (Figure 4C), abdomen (Figure 4D), legs (Figure 4E), and wings (Figure 4F) were reported in the flies at a concentration of 100 and/or 250 µg/ml concentrations graphene or MWCNTs.

3.7 | Phenotypic variations

After treatment of four different concentrations (0.1, 10, 100, and 250 µg/ml) of graphene or MWCNTs, F0 (parent) was obtained, and then, phenotypic variations were examined. Later, *Drosophila* adult individuals belonging to F1, F2, and F3 generations were obtained from F0 individuals. The F1, F2, and F3 generations of *Drosophila* flies contain both normal and defective flies. The results obtained from F0, F1, F2, and F3 generations showed phenotypic variations in the wings and mouths of flies at the two highest concentrations (100 and 250 µg/ml).

For each generation, each application concentration was made three times, and a total of 1,500 flies were observed. Figure 5A shows normal wing phenotype of adult *D. melanogaster*. The phenotypic variations observed in the wings of individuals exposed to graphene or MWCNTs were 34 ± 1.2% (510 adult individuals), 35 ± 0.9% (525 adult individuals), 41 ± 1.8% (615 adult individuals), and 38 ± 1.6% (570 adult individuals) of the total population, respectively (Figure 5B–F). On the other hand, Figure 6A shows normal mouth phenotype of adult flies. The phenotypic variations observed in the mouth of individuals treated with graphene or MWCNTs

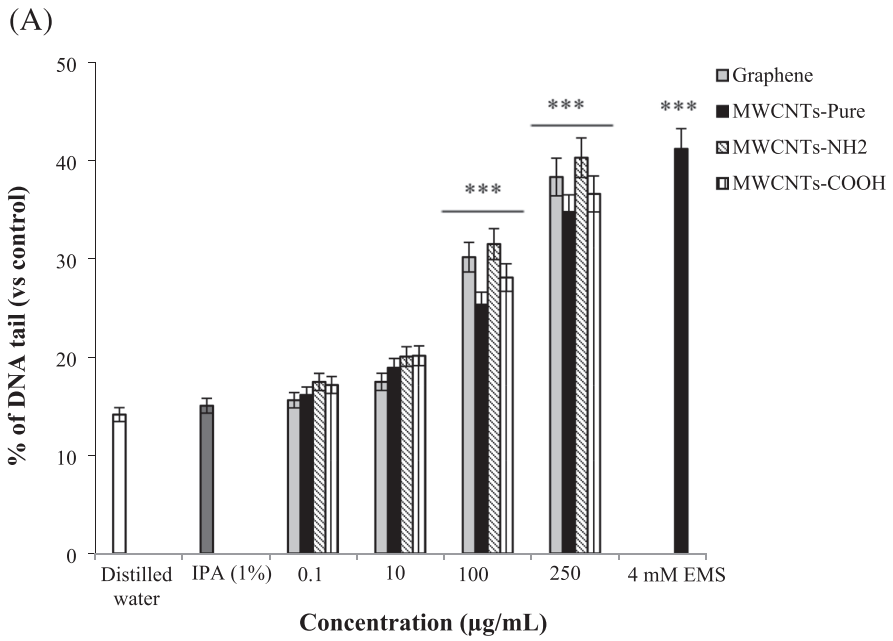

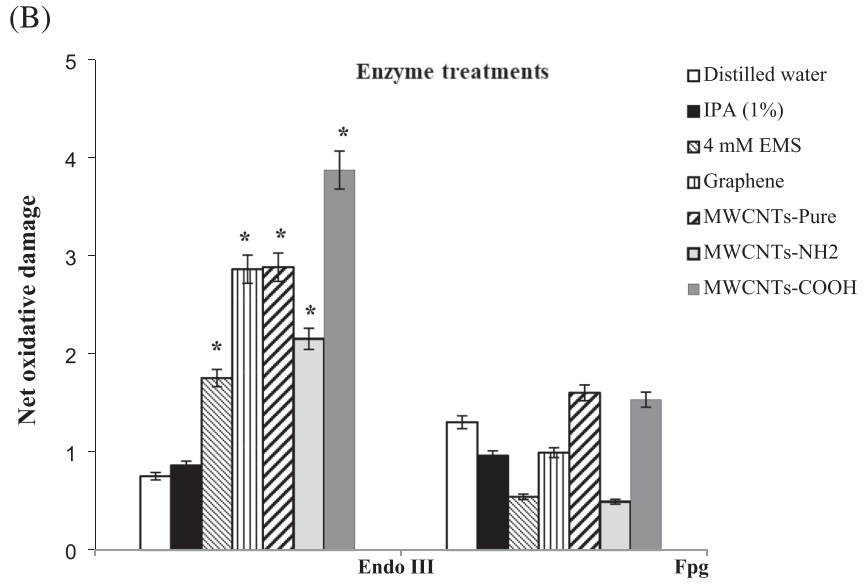

FIGURE 3 Genotoxic effects of graphene or MWCNTs (as pure, amide [NH_2] functionalized and carboxyl [COOH] functionalized) in the comet assay. Results indicate the % of DNA tail induced after the larvae exposed to different concentrations (0.1, 10, 100, and 250 µg/ml) of graphene or WCNTs for 24 h (three replicates were carried out, and 100 randomly selected cells were analyzed per treatment) (a). Net oxidative damage induction in hemocytes after graphene or MWCNTs exposure at the concentration of 250 µg/ml during larvae stage. Effects induced by buffer exposure were subtracted from those obtained after enzyme treatments (Endo III and Fpg) (B). Data represent the mean ± standard error (SE) of the mean. EMS (4 mM) was used as positive control. $^{*}P \leq 0.05$, $^{***}P \leq 0.001$ when compared to the negative control using Student's *t* test

were 39 ± 0.8% (585 adult individuals), 40 ± 1.1% (600 adult individuals), 46 ± 0.5% (690 adult individuals), and 42 ± 1.9% (630 adult individuals) of the total population, respectively (Figure 6B–F).

3.8 | Effect of graphene and MWCNTs exposure on climbing behavior in flies

Impaired climbing ability is generally considered an indication of seriously damaged locomotor behavior in flies. Significant differences were detected in climbing behavior among test and control flies after 7-day exposure to NMs. Locomotor behavior was determined as 92 ± 4.7% in IPA (1%), but the climbing efficiency was highly impaired in the flies exposed to 250 µg/ml of graphene or MWCNTs (56 ± 9.1%), (61 ± 7.3%), (49 ± 8.7%), and (58 ± 9.5%), while those exposed to 100 µg/ml were observed to have even worse climbing efficiency (74 ± 8.4%), (72 ± 3.9%), (68 ± 7.2%), and (70 ± 5.2%) respectively, as compared to controls (100%) (Figure 7). The results indicated that exposure to graphene or MWCNTs induced greater impairment in climbing efficiency in flies depending on the dose exposed, reaching significance at the highest tested concentrations (100 and 250 µg/ml).

3.9 | Detection of parasitoid resistance (or encapsulation assay) and cellular immune response

Graphene or MWCNTs were applied together with two different lines of *L. boulardi* (NSRef and G486), one of the most important natural enemies of *D. melanogaster*, endoparasitoid wasps. A statistically significant increase was observed in the number of capsules,

TABLE 1 Summary of the results obtained in the *drosophila* wing spot test after treatments with graphene

Test compounds (μg/ml)	Number of wings (*N*)	Small single spots (1–2 cells) ($m = 2$)			Large single spots (>2 cells) ($m = 5$)			Twin spots ($m = 5$)			Total *mwh* spots ($m = 2$)			Total spots ($m = 2$)			Frequency of clone formation per 10^5 cells
		No	Fr	D	No	Fr	D	No	Fr	D	No	Fr	D	No	Fr	D	
Marker heterozygous wings (*mwh/flr*^{3})																	
Distilled water	80	12	(0.15)		4	(0.05)		1	(0.01)		17	(0.21)		17	(0.21)		0.87
Isopropanol (IPA, 1%)	80	13	(0.16)	i	2	(0.03)	−	1	(0.01)	i	16	(0.20)	i	16	(0.20)	i	0.82
EMS (1 mM)	80	156	(1.95)	+	29	(0.36)	+	15	(0.19)	+	191	(2.39)	+	200	(2.50)	+	9.78
0.1	80	15	(0.19)	i	1	(0.01)	−	0	(0.00)	i	16	(0.20)	i	16	(0.20)	i	0.82
10	80	19	(0.24)	i	3	(0.04)	i	1	(0.01)	i	23	(0.29)	i	23	(0.29)	i	1.18
100	80	22	(0.28)	i	2	(0.03)	i	1	(0.01)	i	25	(0.31)	i	25	(0.31)	i	1.28
250	80	32	(0.40)	+	9	(0.11)	+	4	(0.05)	i	44	(0.55)	+	45	(0.56)	+	2.25
Balancer heterozygous wings (*mwh/TM3*)																	
Distilled water	80	14	(0.18)		3	(0.04)					17	(0.21)		17	(0.21)		0.87
Isopropanol (IPA, 1%)	80	15	(0.19)	i	3	(0.04)	i				18	(0.23)	i	18	(0.23)	i	0.92
EMS (1 mM)	80	75	(0.94)	+	22	(0.28)	+				90	(1.13)	+	97	(1.21)	+	4.61
0.1	80	13	(0.16)	−	4	(0.05)	i				17	(0.21)	−	17	(0.21)	−	0.87
10	80	16	(0.20)	i	3	(0.04)	i				19	(0.24)	i	19	(0.24)	i	0.97
100	80	20	(0.25)	i	2	(0.03)	−				22	(0.28)	i	22	(0.28)	i	1.13
250	80	24	(0.30)	i	2	(0.03)	−				26	(0.33)	i	26	(0.33)	i	1.33

Note: Probability levels, $\alpha = \beta = 0.05$; a total of 80 wings were scored per concentration.

Abbreviations: D, statistical diagnosis according to H. Frei and Würgler (1988, 1995); Fr, frequency; i: inconclusive; m, multiplicative factor; No, number; −, negative; +, positive.

TABLE 2 Summary of the results obtained in the *drosophila* wing spot test after treatments with MWCNTs-pure

Test compounds (μg/ml)	Number of wings (*N*)	Small single spots (1–2 cells) ($m = 2$)			Large single spots (> 2 cells) ($m = 5$)			Twin spots ($m = 5$)			Total *mwh* spots ($m = 2$)			Total spots ($m = 2$)			Frequency of clone formation per 10^5 cells
		No	Fr	D	No	Fr	D	No	Fr	D	No	Fr	D	No	Fr	D	
Marker heterozygous wings (*mwh/flr*^{3})																	
Distilled water	80	12	(0.15)		4	(0.05)		1	(0.01)		17	(0.21)		17	(0.21)		0.87
Isopropanol (IPA, 1%)	80	13	(0.16)	i	2	(0.03)	−	1	(0.01)	i	16	(0.20)	i	16	(0.20)	i	0.82
EMS (1 mM)	80	156	(1.95)	+	29	(0.36)	+	15	(0.19)	+	191	(2.39)	+	200	(2.50)	+	9.78
0.1	80	14	(0.18)	i	1	(0.01)	−	0	(0.00)	i	15	(0.19)	−	15	(0.19)	−	0.77
10	80	16	(0.20)	i	2	(0.03)	i	1	(0.01)	i	19	(0.24)	i	19	(0.24)	i	0.97
100	80	21	(0.26)	i	1	(0.01)	−	2	(0.03)	i	24	(0.30)	i	24	(0.30)	i	1.23
250	80	30	(0.38)	+	7	(0.09)	i	2	(0.03)	i	39	(0.49)	+	39	(0.49)	+	2.00
Balancer heterozygous wings (*mwh/TM3*)																	
Distilled water	80	14	(0.18)		3	(0.04)					17	(0.21)		17	(0.21)		0.87
Isopropanol (IPA, 1%)	80	15	(0.19)	i	3	(0.04)	i				18	(0.23)	i	18	(0.23)	i	0.92
EMS (1 mM)	80	75	(0.94)	+	22	(0.28)	+				90	(1.13)	+	97	(1.21)	+	4.61
0.1	80	14	(0.18)	−	2	(0.03)	−				16	(0.20)	−	16	(0.20)	−	0.82
10	80	17	(0.21)	i	1	(0.01)	−				18	(0.23)	i	18	(0.23)	i	0.92
100	80	22	(0.28)	i	3	(0.04)	i				25	(0.31)	i	25	(0.31)	i	1.28
250	80	26	(0.33)	i	2	(0.03)	−				28	(0.35)	i	28	(0.35)	i	1.43

Note: Probability levels, $\alpha = \beta = 0.05$; a total of 80 wings were scored per concentration.

Abbreviations: D, statistical diagnosis according to H. Frei and Würgler (1988, 1995); Fr, frequency; i: inconclusive; m, multiplicative factor; No, number; −, negative; +, positive.

TABLE 3 Summary of the results obtained in the *drosophila* wing spot test after treatments with MWCNTs-NH_2

Test compounds (μg/ml)	Number of wings (*N*)	Small single spots (1–2 cells) (*m* = 2)			Large single spots (> 2 cells) (*m* = 5)			Twin spots (*m* = 5)			Total *mwh* spots (*m* = 2)			Total spots (*m* = 2)			Frequency of clone formation per 10^5 cells
		No	Fr	D	No	Fr	D	No	Fr	D	No	Fr	D	No	Fr	D	
Marker heterozygous wings (*mwh/flr*^{3})																	
Distilled water	80	12	(0.15)		4	(0.05)		1	(0.01)		17	(0.21)		17	(0.21)		0.87
Isopropanol (IPA, 1%)	80	13	(0.16)	i	2	(0.03)	−	1	(0.01)	i	16	(0.20)	i	16	(0.20)	i	0.82
EMS (1 mM)	80	156	(1.95)	+	29	(0.36)	+	15	(0.19)	+	191	(2.39)	+	200	(2.50)	+	9.78
0.1	80	15	(0.19)	i	1	(0.01)	−	0	(0.00)	i	15	(0.19)	−	15	(0.19)	−	0.77
10	80	17	(0.21)	i	2	(0.03)	i	1	(0.01)	i	19	(0.24)	i	19	(0.24)	i	0.97
100	80	20	(0.25)	i	1	(0.01)	−	2	(0.03)	i	24	(0.30)	i	24	(0.30)	i	1.23
250	80	33	(0.41)	+	10	(0.13)	+	3	(0.04)	i	46	(0.58)	+	46	(0.58)	+	2.36
Balancer heterozygous wings (*mwh/TM3*)																	
Distilled water	80	14	(0.18)		3	(0.04)					17	(0.21)		17	(0.21)		0.87
Isopropanol (IPA, 1%)	80	15	(0.19)	i	3	(0.04)	i				18	(0.23)	i	18	(0.23)	i	0.92
EMS (1 mM)	80	75	(0.94)	+	22	(0.28)	+				90	(1.13)	+	97	(1.21)	+	4.61
0.1	80	16	(0.20)	i	1	(0.01)	−				17	(0.21)	−	17	(0.21)	−	0.87
10	80	18	(0.23)	i	1	(0.11)	−				19	(0.24)	i	19	(0.24)	i	0.97
100	80	23	(0.29)	i	2	(0.03)	−				25	(0.31)	i	25	(0.31)	i	1.28
250	80	25	(0.31)	i	1	(0.01)	−				26	(0.33)	i	26	(0.33)	i	1.33

Note: Probability levels, $\alpha = \beta = 0.05$; a total of 80 wings were scored per concentration.

Abbreviations: D, statistical diagnosis according to H. Frei and Würgler (1988, 1995); Fr, frequency; i: inconclusive; m, multiplicative factor; No, number; −, negative; +, positive.

TABLE 4 Summary of the results obtained in the *drosophila* wing spot test after treatments with MWCNTs-COOH

Test compounds (μg/ml)	Number of wings (*N*)	Small single spots (1–2 cells) (*m* = 2)			Large single spots (> 2 cells) (*m* = 5)			Twin spots (*m* = 5)			Total *mwh* spots (*m* = 2)			Total spots (*m* = 2)			Frequency of clone formation per 10^5 cells
		No	Fr	D	No	Fr	D	No	Fr	D	No	Fr	D	No	Fr	D	
Marker heterozygous wings (*mwh/flr*^{3})																	
Distilled water	80	12	(0.15)		4	(0.05)		1	(0.01)		17	(0.21)		17	(0.21)		0.87
Isopropanol (IPA, 1%)	80	13	(0.16)	i	2	(0.03)	−	1	(0.01)	i	16	(0.20)	i	16	(0.20)	i	0.82
EMS (1 mM)	80	156	(1.95)	+	29	(0.36)	+	15	(0.19)	+	191	(2.39)	+	200	(2.50)	+	9.78
0.1	80	14	(0.18)	i	1	(0.01)	−	0	(0.00)	i	15	(0.19)	−	15	(0.19)	−	0.77
10	80	16	(0.20)	i	2	(0.03)	i	1	(0.01)	i	19	(0.24)	i	19	(0.24)	i	0.97
100	80	21	(0.26)	i	1	(0.01)	−	2	(0.03)	i	24	(0.30)	i	24	(0.30)	i	1.23
250	80	29	(0.36)	+	9	(0.11)	+	2	(0.03)	i	40	(0.50)	+	40	(0.50)	+	2.05
Balancer heterozygous wings (*mwh/TM3*)																	
Distilled water	80	14	(0.18)		3	(0.04)					17	(0.21)		17	(0.21)		0.87
Isopropanol (IPA, 1%)	80	15	(0.19)	i	3	(0.04)	i				18	(0.23)	i	18	(0.23)	i	0.92
EMS (1 mM)	80	75	(0.94)	+	22	(0.28)	+				90	(1.13)	+	97	(1.21)	+	4.61
0.1	80	15	(0.19)	i	2	(0.03)	−				17	(0.21)	−	17	(0.21)	−	0.87
10	80	19	(0.24)	i	0	(0.00)	−				19	(0.24)	i	19	(0.24)	i	0.97
100	80	24	(0.30)	i	3	(0.04)	i				27	(0.34)	i	27	(0.34)	i	1.38
250	80	26	(0.33)	i	2	(0.03)	−				28	(0.35)	i	28	(0.35)	i	1.43

Note: Probability levels, $\alpha = \beta = 0.05$; a total of 80 wings were scored per concentration.

Abbreviations: D, statistical diagnosis according to H. Frei and Würgler (1988, 1995); Fr, frequency; i: inconclusive; m, multiplicative factor; No, number; −, negative; +, positive.

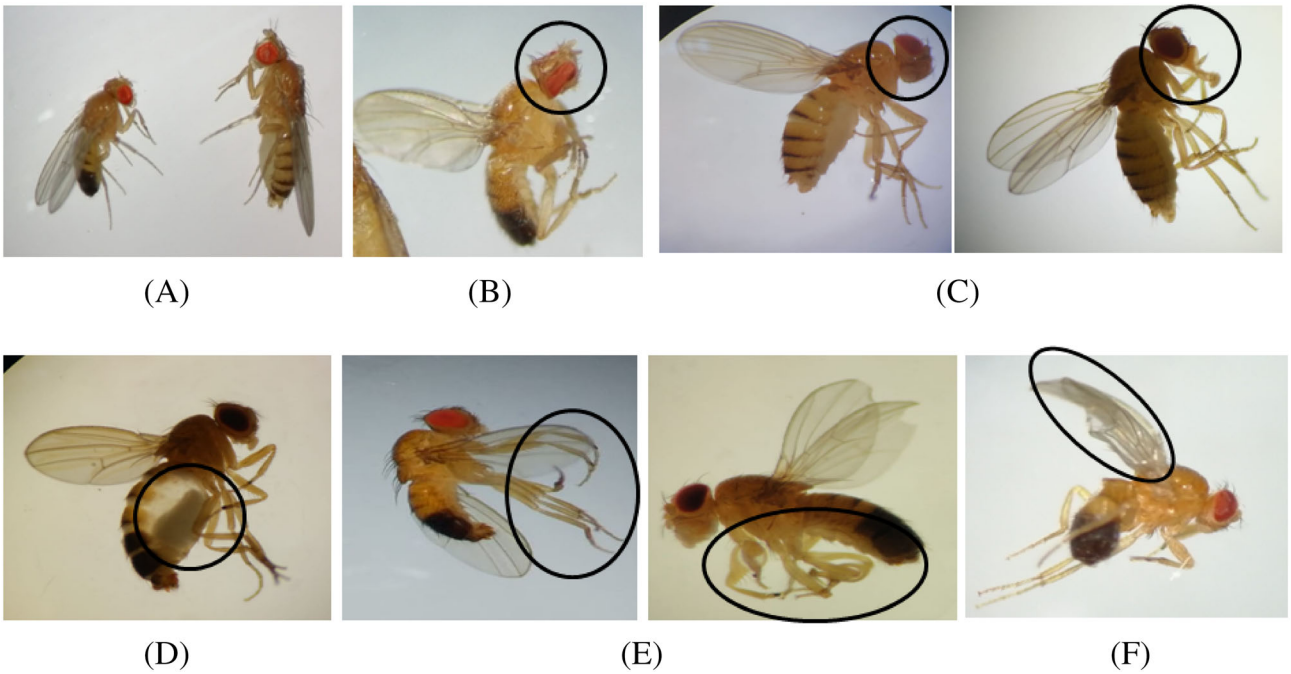

FIGURE 4 Normal phenotypes of adult *D. melanogaster* (a). Morphological alterations in the eye (B), mouth (C), abdomen (D), leg (E), and wing (F) parts of adult *D. melanogaster* observed at 100 and/or 250 μg/ml concentrations of graphene or MWCNTs (as pure, amide [NH_2] functionalized and carboxyl [COOH] functionalized). Black circles indicate the defective area in the image

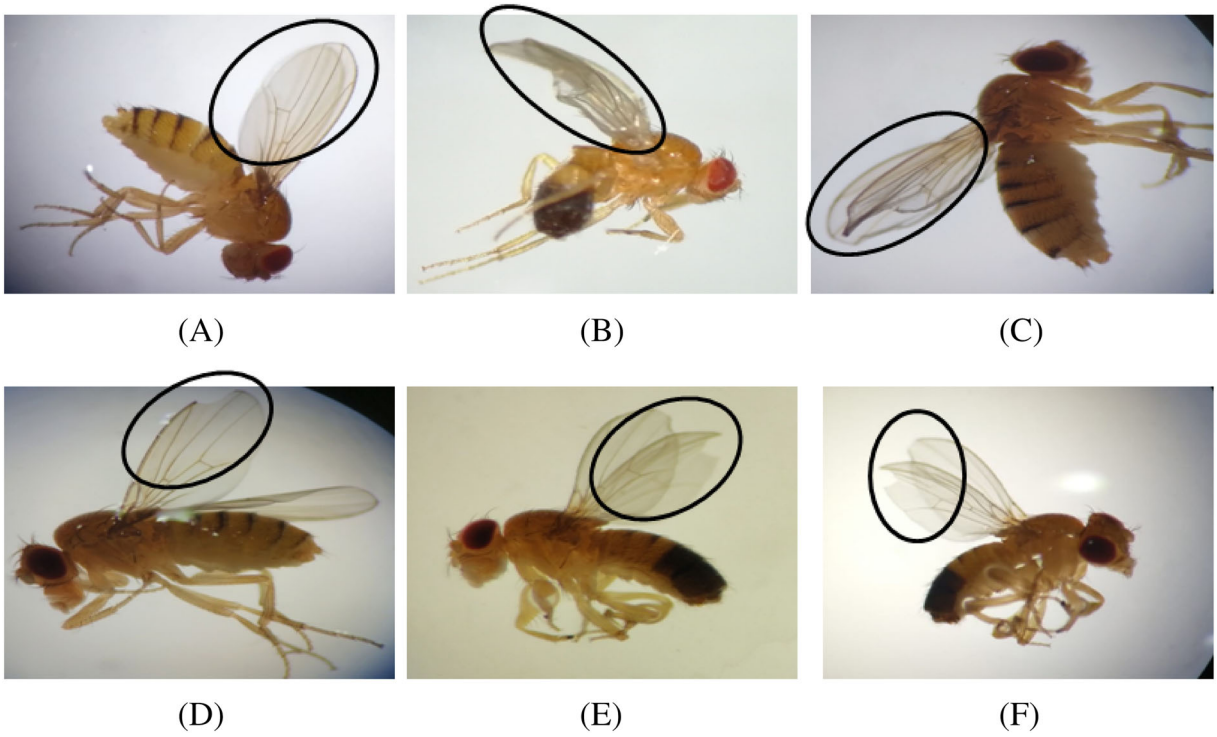

FIGURE 5 Normal wing phenotype (a) and abnormal wing phenotypes (B–F) in F0, F1, F2, and F3 generations obtained after treatment with 100 and 250 μg/ml concentrations of graphene or MWCNTs (as pure, amide [NH_2] functionalized and carboxyl [COOH] functionalized) to *drosophila* larvae. Black circles indicate the defective area in the image

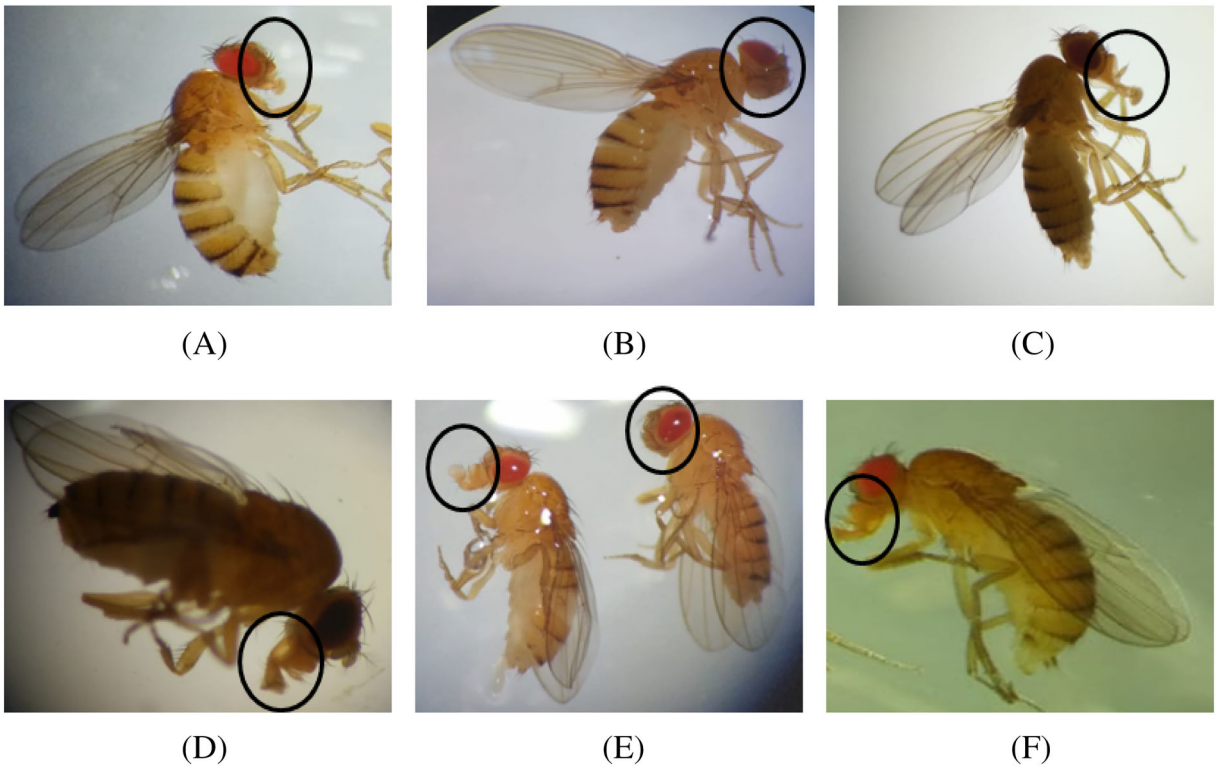

FIGURE 6 Normal mouth phenotype (a) and abnormal mouth phenotypes (B–F) in F0, F1, F2, and F3 generations obtained after treatment with 100 and 250 μg/ml concentrations of graphene or MWCNTs (as pure, amide [NH_2] functionalized and carboxyl [COOH] functionalized) to *drosophila* larvae. Black circles indicate the defective area in the image

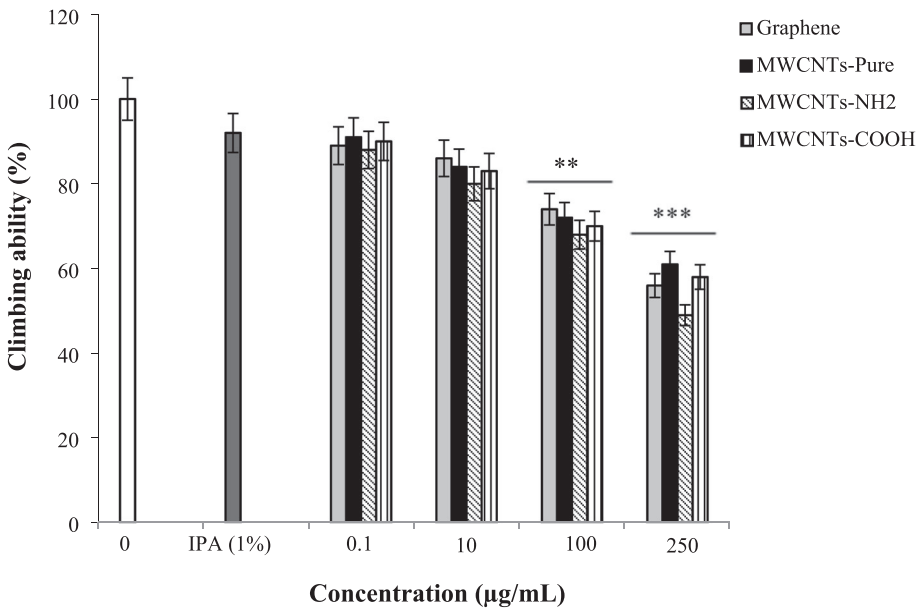

FIGURE 7 Climbing behavior of flies monitored after 7 days of exposure to MWCNTs (as pure, amide [NH_2] functionalized and carboxyl [COOH] functionalized) recorded after 10 s. data represent the mean ± standard error (SE) of the mean. $^{**}P \leq 0.01$, $^{***}P \leq 0.001$ when compared to the negative control using one way ANOVA

encapsulation rate and capsule rate at 250 μg/ml of graphene or MWCNTs (Tables S5–S8). Considering the number of infected flies, number of capsules, encapsulation rate, and capsule rate, MWCNTs-NH_2 treatment is more effective than other NMs.

Total hemocyte counts were investigated after treatment of graphene or MWCNTs and *L. boulardi* (NSRef and G486) to *Drosophila* larvae (48 ± 4 h). NSRef and G486 treatment with the highest concentration of graphene or MWCNTs (250 μg/mL) showed an increase in the number of hemocyte compared to the group that only NM treated (Figure 8A–D).

Proportions of lamellocytes and plasmatocytes were investigated after treatment of graphene or MWCNTs and *L. boulardi* (NSRef and

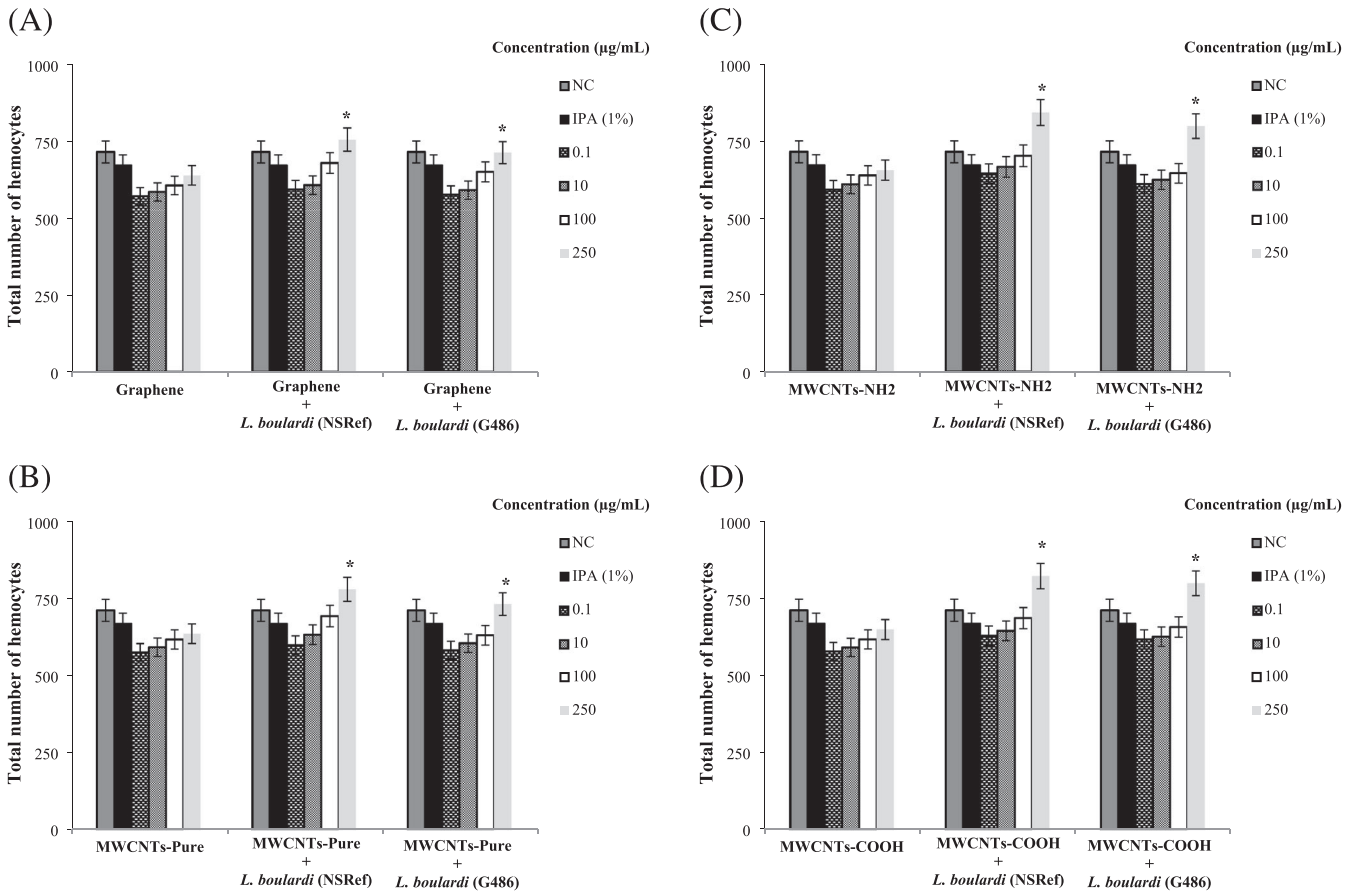

FIGURE 8 Total number of hemocytes data obtained after treatment with graphene or MWCNTs (as pure, amide [NH_2] functionalized and carboxyl [COOH] functionalized) in combination with *Leptopilina boulardi* (NSRef or G486) to 48-hour *drosophila* larvae (A-D). $^{*}P \leq 0.05$ graphene or MWCNTs+*L. boulardi* (NSRef or G486) treatment compared to graphene or MWCNTs (Mann–Whitney *U* test)

G486) to *Drosophila* larvae (48 ± 4 h). A significant increase in the number of lamellocytes at 250 µg/ml was observed after endoparasite infection, depending on the concentration. The increase in *L. boulardi* (NSRef) infection along with NM application is higher than *L. boulardi* (G486) (Figure 9A,C,E,G). On the other hand, graphene or MWCNTs did not induce significant increases in the proportion of plasmatocytes (Figure 9B,D,F,H). Figure 9I represents infected *D. melanogaster* larvae and adult with *L. boulardi* (NSRef or G486).

4 | DISCUSSION

Humans and other vertebrates have an innate defense system as the first line of defense to fight microbial pathogens like viruses before the acquired immune system is triggered. Thanks to the remarkable homology between humans and *Drosophila* innate immune mechanisms, these flies have recently been used in research into our immune response to infection. Although they do not possess an adaptive immune system like all invertebrates but only innate immune mechanism composed of circulating hemocytes, *Drosophila* flies fight pathogens through a series of defensive reactions. This makes it an ideal model to investigate characteristics of human innate immune system that could otherwise be overshadowed by adaptive immune system. The three mature hemocyte types are the plasmatocytes, crystal cells, and lamellocytes are known to work together to mediate the *Drosophila* immune response against parasitoid infection. During the immune response against parasitoids in *Drosophila*, three types of hemocytes are mobilized, which include lamellocytes, crystal cells, and plasmatocytes (Leitão et al., 2019; Lemaitre & Hoffmann, 2007). *Drosophila*'s immune defense against parasites triggers a specialized cellular response known as encapsulation, which relies on the three different types of mature blood cells (Lavine & Strand, 2002; Leitão & Sucena, 2015). In order to generate lamellocytes, crystal cells, and plasmatocytes, *Drosophila* hemocytes rapidly begin to differentiate in the case of infection (Kraaijeveld et al., 2001).

Plasmatocytes are phagocytic and analogous to human macrophages and engulf small particles and bacteria while transforming into lamellocytes. The most abundant hemocyte is the plasmatocyte, comprising approximately 90–95% of total hemocytes in the healthy larva (Gold & Brückner, 2015; Honti et al., 2014; Letourneau et al., 2016). They do however play a key role in the fight against parasitoid infection as the first cells to adhere to the parasitoid egg to form the primary layer of encapsulating cells linked together with tight junctions

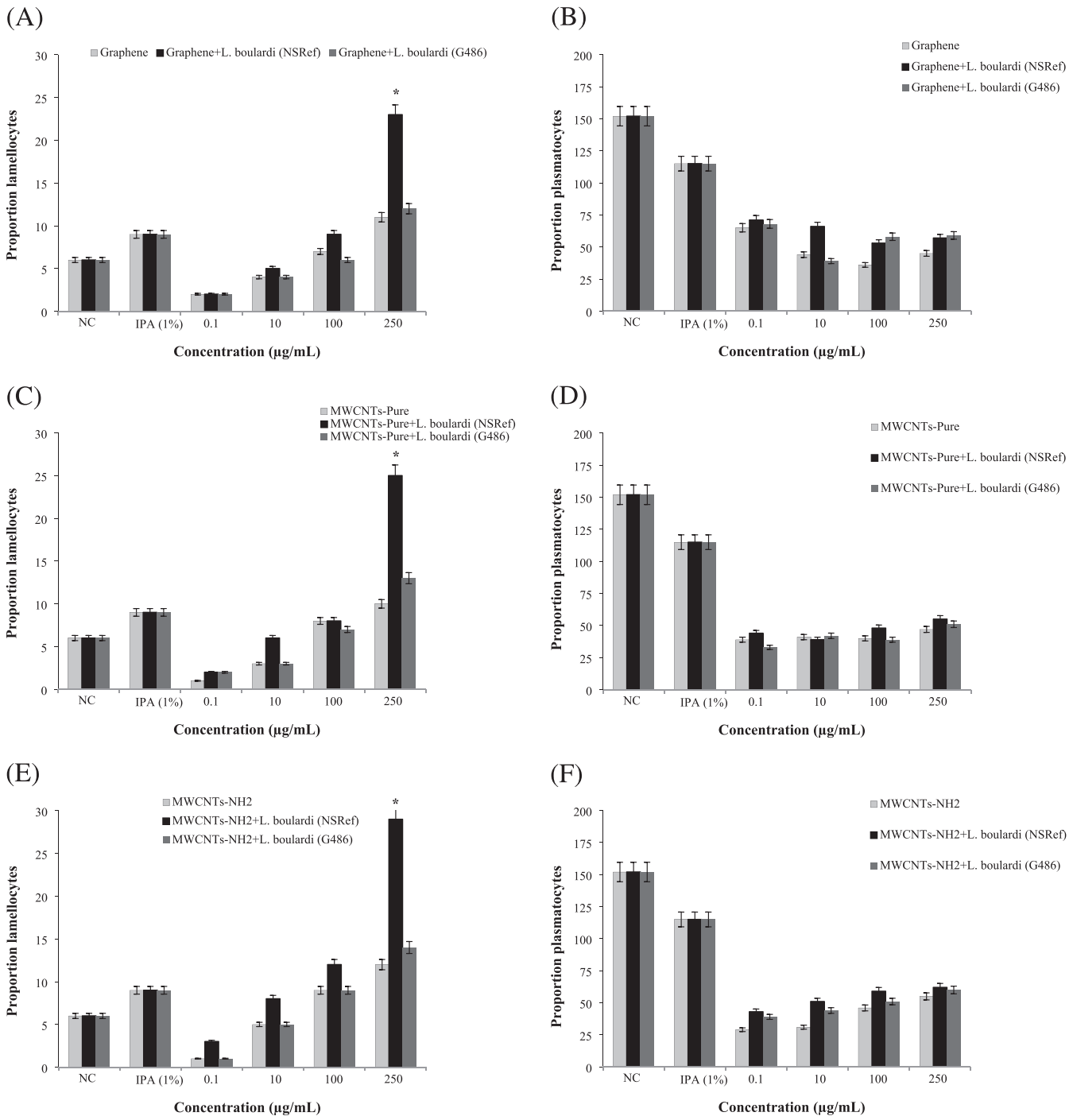

FIGURE 9 Proportions of lamellocytes and plasmatocytes data obtained after treatment with graphene or MWCNTs (as pure, amide [NH_2] functionalized and carboxyl [COOH] functionalized) in combination with *Leptopilina boulardi* (NSRef or G486) to 48-hour *drosophila* larvae (A–H). Infected *D. melanogaster* larvae and adult individual (I). Black circles indicate parasitoid wasps encapsulated in *D. melanogaster*. $^{*}P \leq 0.05$ graphene or MWCNTs+*L. boulardi* (NSRef or G486) treatment compared to graphene or MWCNTs (Mann–Whitney *U* test)

(Honti et al., 2014). Lamellocytes are large cells encapsulating foreign bodies, such as parasitoid eggs, just like human platelet clotting. Lamellocytes are the least abundant cell type in healthy larvae, rarely seen in uninfected larvae and never seen in embryos or adult flies (Jalvingh et al., 2014), but are generated in large numbers upon parasitoid infection (Lanot et al., 2001). Once adhered to the parasitoid egg, lamellocytes recruit crystal cells to the site, melanizing and killing the egg in an oxidative burst. Lamellocytes produce one of the three polyphenoloxidases (PPO) found in the *Drosophila* genome in order to fully melanize the capsule (Dudzic et al., 2015). If the encapsulation is not fast enough, or the response is impaired or overwhelmed, wasp larvae are most likely to kill their host (Strand, 2008). No studies in

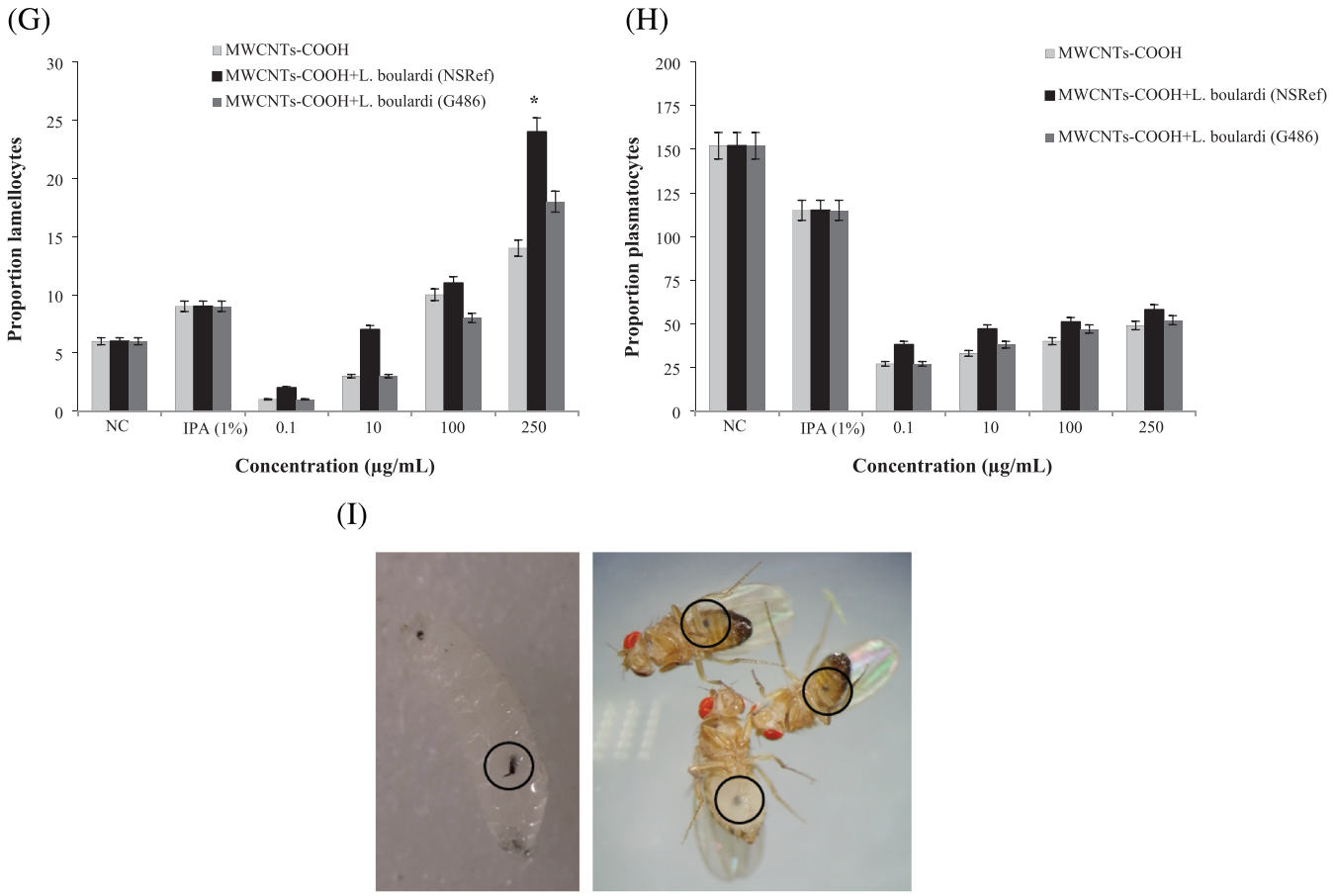

FIGURE 9 (Continued)

D. melanogaster have tested the parasitoid resistance, and cellular immune response of graphene or MWCNTs exposure along with *L. boulardi* (NSRef and G486) infection. An important aspect of this study was the use of parasitoid wasps to determine immune response and resistance. This is the first study to evaluating the immune-nanotoxicity potential of graphene or MWCNTs using *D. melanogaster*. At the highest concentration (250 µg/ml) of graphene and MWCNT (as pure, NH2 functionalized, and COOH functionalized) did inducesignificant effects in the number of hemocytes, especially lamellocytes.

It is vital to understand immune compatibility before NMs are consumed and used in clinical settings. This can only be achieved by determining NM-induced immune toxicity using in vitro and in vivo testing. However, there are some difficulties in selecting an appropriate model and endpoint for in vitro testing. More specifically, the selection of positive and negative controls to employ could be a complicated decision, and predictability of immune-nanotoxicity in in vivo tests is inherently difficult. Therefore, it is known that standard in vivo toxicity screens afford low sensitivity in determining immune nanotoxicity. Extensive breeding periods in mammals, high costs, and growing ethical concerns have been restricting widespread use of mammals as test models in immune nanotoxicity experiments. *D. melanogaster*, on the other hand, offers a versatile and dynamic tool with a huge potential to accelerate research into toxic impact of NMs on the immune system (Demir, 2020c; Demir & Marcos, 2017, 2018a; Ng et al., 2019). Previous studies have shown that NMs may cause some serious adverse effects on the immune system, but despite its advantages, there is still little research to explore immune toxicity of NMs using *D. melanogaster*. Despite the structural differences, the degree of biological and physiological protection makes *Drosophila* a valuable model in nanotoxicology (Pappus & Mishra, 2018; Vecchio, 2015).

Graphene oxide (GO) widely used in biotechnological fields and medical applications. GO is attracting great attention; however, its long-term effects on organisms have yet to be characterized. To that end, researchers have been conducting studies to discover possible effects of GO NPs using model organisms. One of these studies evaluated in vivo toxicity of GO NPs in *D. melanogaster* after oral administration, finding that these NPs can induce developmental delay and reduce adult hatching and that the toxicity of GO could be associated with production of oxidative stress (Zou et al., 2016). Their longevity assay results suggested that GO NPs caused little adverse effects in the longevity of flies. One study examined the impacts of different doses of dietary GO nanosheets on the development of *D. melanogaster*. They found that the exposure led to significant changes in the crawling speed and trailing path during the larval

stage, as well as production of ROS in the larval hemolymph, DNA damage, impaired phototactic and geotactic behavior in adult flies. Furthermore, researchers observed phenotypic defects in the wings, eyes, thorax bristles, and mouths of the flies (Priyadarsini et al., 2019). Three-dimensional nanocomposites produced from two-dimensional GO nanoplatelets and oxide materials have been reported to exhibit improved mechanical and biological properties, with favorable cell viability when tested in *D. melanogaster* (Kumar et al., 2019). More recent research compared the in vivo toxicity of GO NPs and ZnO NPs using different assays such as mortality, MTT, larval crawling, and climbing screens, as well as analyses of protein content. GO NPs were found to induce less cytotoxicity, while ZnO NPs impaired the neuromuscular coordination as a neurotoxic effect (Sood et al., 2019). All these findings are in agreement with the results in *D. melanogaster* showing that the induced somatic recombination detected in the SMART, elevated ROS production, DNA damage, alteration in locomotor ability increased significantly with concentration of graphene.

Plenty of previous work in the relevant literature looked into possible detrimental impact of CNTs in *Drosophila* flies, while only two studies have so far deal examined their genotoxic effects in vivo. In the first study, the researchers exposed *Drosophila* larvae to SWCNTs and studied their biodistribution in several larval compartments and found that CNTs had no significant impact on the viability of larvae (Leeuw et al., 2007). MWCNTs, on the other hand, were found to adhere weakly failing to cause a marked impairment in locomotor function or survival (Liu et al., 2009). The lack of toxicity of SWCNT exposure was also confirmed by a study that reported no effects on larval growth and viability (Philbrook et al., 2011). One study used a different exposure approach by injecting CNTs into *Drosophila* embryos rather than including them in food medium and observed that MWCNTs no verifiable effects on cell motility, tissue and organ formation, cell communication, and embryo viability (Liu et al., 2014). Despite these reports, seemingly contradicting findings noted that CNT exposure by injection caused significant mortality; however, SWCNTs at lower doses were found to exert greater toxic effects than MWCNT exposure (Vega-Alvarez et al., 2014). All these studies suggest that *Drosophila* embryos might be an ideal model in NM toxicity testing. Overall, these toxicity findings from *Drosophila* research seem to corroborate the common view that SWCNTs in terms of aspect ratio exert more detrimental effects than those caused by MWCNTs (Jia et al., 2005).

As for the genotoxicity of CNTs in *Drosophila*, only two studies have so far used the wing spot assay to measure somatic mutation and recombination upon NM exposure. They reported negative results for MWCNTs in agreement the current scientific opinion that MWCNTs had no genotoxicity at reported exposure doses in high metabolic efficiency strains (Machado et al., 2013) or standard strains of flies (de Andrade et al., 2014). Lastly, a recent study examined the toxicity of candle soot derived CNTs through an in vivo assay in *Drosophila* flies and found no toxic effects (Pandey et al., 2019). In this study, the results obtained from trans-heterozygous wings (*mwh/flr*^{3}) exposure to 250 μg/ml concentrations of the MWCNTs (as pure, NH2 functionalized, and COOH functionalized) demonstrated clearly positive results for small single spots, large single spots, total *mwh* spots, and total spots. The results obtained current study showed that the MWCNTs at higher concentrations were potentially genotoxic via the induction of somatic recombination.

5 | CONCLUSION

This has been the first study to use *D. melanogaster* as an in vivo model to examine the nanotoxicity, nanogenotoxicity, immune-nanotoxicity, phenotypic variations, locomotor behavior, morphological defects, parasitoid resistance, and cellular immune response upon exposure to graphene or MWCNTs. The results once again validated *D. melanogaster* as a dynamic in vivo model to explore possible risks and effects of these NMs. However, since such studies are directly related to human and environmental health, future toxicity testing and studies are warranted to confirm the reliability of various systems (in vivo and in vitro research) and model organisms to explain of the molecular mechanisms triggered by exposure to NMs. The main points of the foregoing discussion could be summarized as follows:

1. These samples were not contaminated with endotoxins.
2. The NMs did induce significant cytotoxic effects at doses lower than 250 μg/ml.
3. There were notable changes in intracellular ROS production, primary DNA damage, and oxidative DNA damage after exposure to concentrations of 100 and/or 250 μg/ml.
4. The largest dose of NMs (250 μg/ml) was found to exert genotoxic impact in the wing-spot assay by inducing somatic recombination.
5. The NMS induced elevated concentration-dependent climbing efficiency (or locomotor behavior) in flies, reaching significance at the highest tested concentrations (100 and 250 μg/ml).
6. A statistically significant increase was observed in the number of capsules and encapsulation rate at the dose of 250 μg/ml.
7. *L. boulardi* strains (NSRef and G486) treatment with the highest concentration of the NMs (250 μg/ml) showed an increase in the number of hemocyte compared to the group that only NM treated.
8. A significant increase in the number of lamellocytes at 250 μg/ml was observed after endoparasite infection depending on the concentration. The increase in *L. boulardi* (NSRef) infection along with NM application is higher than *L. boulardi* (G486).
9. A morphological defect in the eyes, mouths, abdomens, legs, and wings of the flies were observed at two largest doses (100 and/or 250 μg/ml).
10. Phenotypic variations were detected in the wings and mouths of F0, F1, F2, and F3 generations at the two largest doses (100 and 250 μg/ml) of NM exposure.

ACKNOWLEDGEMENT

This research is supported by the Scientific and Technical Research Council of Turkey (Türkiye Bilimsel ve Teknolojik Araştırma Kurumu, TUBITAK) (Project ID: 218Z031), Ankara (Turkey).

AUTHOR CONTRIBUTIONS

Laboratory experiments, data collection, writing-original draft and funding acquisition were conducted by Eşref Demir.

CONFLICT OF INTEREST

The author declare that he has no known competing financial interests or personal relationships that could has appeared to influence the work reported in this paper.

ORCID

Eşref Demir https://orcid.org/0000-0002-2146-7385

REFERENCES

Abraham, S. K. (1994). Antigenotoxicity of coffee in the *drosophila* assay for somatic mutation and recombination. *Mutagenesis*, *9*, 383–386. https://doi.org/10.1093/mutage/9.4.383

Aillon, K. L., Xie, Y., El-Gendy, N., Berkland, C. J., & Forrest, M. L. (2009). Effects of nanomaterial physicochemical properties on in vivo toxicity. *Advanced Drug Delivery Reviews*, *61*, 457–466. https://doi.org/10.1016/j.addr.2009.03.010

Alaraby, M., Annangi, B., Marcos, R., & Hernández, A. (2016). *Drosophila melanogaster* as a suitable in vivo model to determine potential side effects of nanomaterials: A review. *Journal of Toxicology and Environmental Health B Critical Reviews*, *19*, 65–104. https://doi.org/10.1080/10937404.2016.1166466

Anand, A. S., Prasad, D. N., Singh, S. B., & Kohli, E. (2017). Chronic exposure of zinc oxide nanoparticles causes deviant phenotype in *Drosophila melanogaster*. *Journal of Hazardous Materials*, *327*, 180–186. https://doi.org/10.1016/j.jhazmat.2016.12.040

Aqel, A., Abou El-Nour, K. M. M., Ammar, R. A. A., & Al-Warthan, A. (2012). Carbon nanotubes, science and technology part (I) structure, synthesis and characterisation. *Arab Journal Chemical*, *5*, 1–23. https://doi.org/10.1016/j.arabjc.2010.08.022

Asakura, M., Sasaki, T., Sugiyama, T., Takaya, M., Koda, S., Nagano, K., Arito, H., & Fukushima, S. (2010). Genotoxicity and cytotoxicity of multi-wall carbon nanotubes in cultured Chinese hamster lung cells in comparison with chrysotile a fibers. *Journal of Occupational Health*, *52*, 155–166. https://doi.org/10.1539/joh.L9150

Bianco, A., Cheng, H., Enoki, T., Gogotsi, Y., Hurt, R., Koratkar, N., Kyotani, T, Monthioux, M., Park, C., Tascon, J., & Zhang, J. (2013). All in the graphene family - A recommended nomenclature for two-dimensional carbon materials. *Carbon*, *65*, 1–6.

Bianco, A., Kostarelos, K., & Prato, M. (2005). Applications of carbon nanotubes in drug delivery. *Current Opinion in Chemical Biology*, *9*, 674–679. https://doi.org/10.1016/j.cbpa.2005.10.005

Bier, E. (2005). Drosophila, the golden bug, emerges as a tool for human genetics. *Nature Reviews Genetics*, *6*, 9–23. https://doi.org/10.1038/nrg1503

Chatterjee, N., Eom, H. J., & Choi, J. (2014). Effects of silver nanoparticles on oxidative DNA damage-repair as a function of p38 MAPK status: A comparative approach using human Jurkat T cells and the nematode *Caenorhabditis elegans*. *Environmental and Molecular Mutagenesis*, *55*, 122–133. https://doi.org/10.1002/em.21844

Chatterjee, N., Yang, J., & Kim, H. M. (2014). Potential toxicity of differential functionalized multiwalled carbon nanotubes (MWCNT) in human cell line (BEAS2B) and *Caenorhabditis elegans*. *Journal of Toxicology and Environmental Health a*, *77*, 1399–1408. https://doi.org/10.1080/15287394.2014.951756

Contreras, E. Q., Cho, M., Zhu, H., Puppala, H. L., Escalera, G., Zhong, W., & Colvin, V. L. (2012). Toxicity of quantum dots and cadmium salt to *Caenorhabditis elegans* after multigenerational exposure. *Environmental Science & Technology*, *47*, 1148–1154.

de Andrade, L. R., Brito, A. S., de Souza Melero, A. M. G., Zanin, H., Ceragioli, H. J., Baranauskas, V., … Irazusta, S. P. (2014). Absence of mutagenic and recombinagenic activity of multi-walled carbon nanotubes in the *drosophila* wing-spot test and *Allium cepa* test. *Ecotoxicology and Environmental Safety*, *99*, 92–97. https://doi.org/10.1016/j.ecoenv.2013.10.013

Dedeh, A., Ciutat, A., Treguer-Delapierre, M., & Bourdineaud, J. P. (2015). Impact of gold nanoparticles on zebrafish exposed to a spiked sediment. *Nanotoxicology*, *9*, 71–80. https://doi.org/10.3109/17435390.2014.889238

Demir, E. (2020a). *Drosophila* as a model for assessing nanopesticide toxicity. *Nanotoxicology*, *14*, 1271–1279. https://doi.org/10.1080/17435390.2020.1815886

Demir, E. (2020b). A review on nanotoxicity and nanogenotoxicity of different shapes of nanomaterials. *Journal of Applied Toxicology*, *41*, 118–147.

Demir, E. (2020c). An *in vivo* study of nanorod, nanosphere, and nanowire forms of titanium dioxide using *Drosophila melanogaster*: Toxicity, cellular uptake, oxidative stress, and DNA damage. *Journal of Toxicology and Environmental Health a*, *83*, 456–469. https://doi.org/10.1080/15287394.2020.1777236

Demir, E., Aksakal, S., Turna, F., Kaya, B., & Marcos, R. (2015). *In vivo* genotoxic effects of four different nano-sizes forms of silica nanoparticles in *Drosophila melanogaster*. *Journal of Hazardous Materials*, *283*, 260–266. https://doi.org/10.1016/j.jhazmat.2014.09.029

Demir, E., & Marcos, R. (2017). Assessing the genotoxic effects of two lipid peroxidation products (4-oxo-2-nonenal and 4-hydroxy-hexenal) in haemocytes and midgut cells of *Drosophila melanogaster* larvae. *Food and Chemical Toxicolog*, *105*, 1–7. https://doi.org/10.1016/j.fct.2017.03.036

Demir, E., & Marcos, R. (2018a). Antigenotoxic potential of boron nitride nanotubes. *Nanotoxicology*, *12*, 868–884. https://doi.org/10.1080/17435390.2018.1482379

Demir, E., & Marcos, R. (2018b). Toxic and genotoxic effects of graphene and multi-walled carbon nanotubes. *Journal of Toxicology and Environmental Health Part a*, *81*, 645–660. https://doi.org/10.1080/15287394.2018.1477314

Demir, E., Qin, T., Li, Y., Zhang, Y., Guo, X., Ingle, T., Yan, J., Orza, A. I., Biris, A. S., Ghorai, S., Zhou, T., & Chen, T. (2020). Cytotoxicity and genotoxicity of cadmium oxide nanoparticles evaluated using *in vitro* assays. *Mutation Research-Genetic Toxicology and Environmental Mutagenesis*, *850-851*, 503149. https://doi.org/10.1016/j.mrgentox.2020.503149

Demir, E., Turna, F., Aksakal, S., Kaya, B., & Marcos, R. (2014). Genotoxicity of different sweeteners in *drosophila*. *Fresenius Environmental Bulletin*, *23*, 3426–3432.

Demir, E., Turna, F., Vales, G., Kaya, B., Creus, A., & Marcos, R. (2013). *In vivo* genotoxicity assessment of titanium, zirconium and aluminium nanoparticles, and their microparticulated forms, in *drosophila*. *Chemosphere*, *93*, 2304–2310. https://doi.org/10.1016/j.chemosphere.2013.08.022

Donaldson, K., Murphy, F. A., Duffin, R., & Poland, C. A. (2010). Asbestos, carbon nanotubes and the pleural mesothelium: A review and the hypothesis regarding the role of long fibre retention in the parietal pleura, inflammation and mesothelioma. *Particle and Fibre Toxicology*, *7*, 5. https://doi.org/10.1186/1743-8977-7-5

Dreher, K. L. (2004). Health and environmental impact of nanotechnology: Toxicological assessment of manufactured nanoparticles. *Toxicological Sciences*, *77*, 3–5. https://doi.org/10.1093/toxsci/kfh041

Dresselhaus, M. S., Dresselhaus, G., & Jorio, A. (2004). Unusual properties and structure of carbon nanotubes. *Annual Review of Materials Research*, *34*, 247–278. https://doi.org/10.1146/annurev.matsci.34.040203.114607

Dudzic, J. P., Kondo, S., Ueda, R., Bergman, C. M., & Lemaitre, B. (2015). *Drosophila* innate immunity: Regional and functional specialization of prophenoloxidases. *BMC Biology*, *13*, 81. https://doi.org/10.1186/s12915-015-0193-6

Dupas, S., Frey, F., & Carton, Y. (1998). A single parasitoid segregating factor controls immune suppression in drosophila. *Journal of Heredity*, *89*, 306–311. https://doi.org/10.1093/jhered/89.4.306

Frei, H., & Würgler, F. E. (1988). Statistical methods to decide whether mutagenicity test data from *drosophila* assays indicate a positive, negative, or inconclusive results. *Mutation Research*, *203*, 297–308. https://doi.org/10.1016/0165-1161(88)90019-2

Frei, H., & Würgler, F. E. (1995). Optimal experimental design and sample size for the statistical evaluation of data from somatic mutation and recombination tests (SMART) in drosophila. *Mutation Research*, *334*, 247–258. https://doi.org/10.1016/0165-1161(95)90018-7

Godfray, H. C. J. (1994). *Parasitoids : Behavioral and evolutionary ecology*. Princeton University Press. https://doi.org/10.1515/9780691207025

Godwin, H., Nameth, C., Avery, D., Bergeson, L. L., Bernard, D., Beryt, E., Boyes, W., Brown, S., Clippinger, A. J., Cohen, Y., Doa, M., Hendren, C. O., Holden, P., Houck, K., Kane, A. B., Klaessig, F., Kodas, T., Landsiedel, R., Lynch, I., … Nel, E. (2015). Nanomaterial categorization for assessing risk potential to facilitate regulatory decision-making. *ACS Nano*, *9*, 3409–3417. https://doi.org/10.1021/acsnano.5b00941

Golbamaki, N., Rasulev, B., Cassano, A., Marchese Robinson, R. L., Benfenati, E., Leszczynski, J., & Cronin, M. T. D. (2015). Genotoxicity of metal oxide NMs: Review of recent data and discussion of possible mechanisms. *Nanoscale*, *7*, 2154–2198. https://doi.org/10.1039/C4NR06670G

Gold, K. S., & Brückner, K. (2015). Macrophages and cellular immunity in *Drosophila melanogaster*. *Seminars in Immunology*, *27*, 357–368. https://doi.org/10.1016/j.smim.2016.03.010

Graf, U., Würgler, F. E., Katz, A. J., Frei, H., Juan, H., Hall, C. B., & Kale, P. G. (1984). Somatic mutation and recombination test in *Drosophila melanogaster*. *Environmental Mutagenesis*, *6*, 153–188. https://doi.org/10.1002/em.2860060206

Guo, N. L., Wan, Y. W., Denvir, J., Porter, D. W., Pacurari, M., Wolfarth, M. G., Castranova, V., & Qian, Y. (2012). Multiwalled carbon nanotube-induced gene signatures in the mouse lung: Potential predictive value for human lung cancer risk and prognosis. *Journal of Toxicology and Environmental Health Part a*, *75*, 1129–1153. https://doi.org/10.1080/15287394.2012.699852

Hartmann, N. B., Jensen, K. A., Baun, A., Rasmussen, K., Rauscher, H., Tantra, R., Cupi, D., Gilliland, D., Pianella, F., & Riego Sintes, J. M. (2015). Techniques and protocols for dispersing nanoparticle powders in aqueous media—Is there a rationale for harmonization? *Journal Toxicogical Environment Health Part B*, *18*, 299–326. https://doi.org/10.1080/10937404.2015.1074969

Hawkins, A. D., Hawkins, A. D., Thornton, C., Kennedy, A. J., Bu, K., Cizdziel, J., … Willett, K. L. (2015). Gill histopathologies following exposure to nanosilver or silver nitrate. *Journal of Toxicology and Environmental Health Part a*, *78*, 301–315. https://doi.org/10.1080/15287394.2014.971386

He, X., Aker, W. G., & Hwang, H. M. (2014). An *in vivo* study on the photo-enhanced toxicities of S-doped TiO_2 nanoparticles to zebrafish embryos (*Danio rerio*) in terms of malformation, mortality, rheotaxis dysfunction, and DNA damage. *Nanotoxicology*, *8*, 185–195. https://doi.org/10.3109/17435390.2013.874050

Hiroyasu, A., Dewitt, D. C., & Goodman, A. G. (2018). Extraction of hemocytes from *Drosophila melanogaster* larvae for microbial infection and analysis. *Journal of Visualized Experiments*, *135*, 57077.

Hirsch, A. (2002). Functionalization of single-walled carbon nanotubes. *Angewandte Chemie International Edition*, *41*, 1853–1859. https://doi.org/10.1002/1521-3773(20020603)41:11<1853::AID-ANIE1853>3.0.CO;2-N

Honti, V., Csordás, G., Kurucz, É., Márkus, R., & Andó, I. (2014). The cell-mediated immunity of *Drosophila melanogaster*: Hemocyte lineages, immune compartments, microanatomy and regulation. *Developmental and Comparative Immunology*, *42*, 47–56. https://doi.org/10.1016/j.dci.2013.06.005

Hu, X., & Zhou, Q. (2013). Health and ecosystem risks of graphene. *Chemical Reviews*, *113*, 3815–3835. https://doi.org/10.1021/cr300045n

Hunt, P. R., Marquis, B. J., Tyner, K. M., Conklin, S., Olejnik, N., Nelson, B. C., & Sprando, R. L. (2013). Nanosilver suppresses growth and induces oxidative damage to DNA in *Caenorhabditis elegans*. *Journal of Applied Toxicology*, *33*, 1131–1142. https://doi.org/10.1002/jat.2872

Iijima, S. (1991). Helical microtubules of graphitic carbon. *Nature*, *354*, 56–58. https://doi.org/10.1038/354056a0

Jacobsen, N. R., Pojano, G., Wallin, H., & Jensen, K. A. (2010). Nanomaterial dispersion protocol for toxicological studies in ENPRA. Internal ENPRA report. March 2010. National Research Centre for the Working Environment, p. 8.

Jalvingh, K. M., Chang, P. L., Nuzhdin, S. V., & Wertheim, B. (2014). Genomic changes under rapid evolution: Selection for parasitoid resistance. *Proceedings of the Royal Society B: Biological Sciences*, *281*, 20132303. https://doi.org/10.1098/rspb.2013.2303

Jennings, B. H. (2011). *Drosophila* a versatile model in biology & medicine. *Materials Today*, *14*, 190–195. https://doi.org/10.1016/S1369-7021(11)70113-4

Jia, G., Wang, H., Yan, L., Wang, X., Pei, R., Yan, T., Zhao, Y., & Guo, X. (2005). Cytotoxicity of carbon nanomaterials: Single-wall nanotube, multi-wall nanotube, and fullerene. *Environmental Science & Technology*, *39*, 1378–1383. https://doi.org/10.1021/es048729l

Kastenbaum, M. A., & Bowman, K. O. (1970). Tables for determining the statistical significance of mutation frequencies. *Mutation Research*, *9*, 527–549. https://doi.org/10.1016/0027-5107(70)90038-2

Kermanizadeh, A., Gosens, I., MacCalman, L., Johnston, H., Danielsen, P. H., Jacobsen, N. R., Lenz, A. G., Fernandes, T., Schins, R. P. F., Cassee, F. R., Wallin, H., Kreyling, W., Stoeger, T., Loft, S., Møller, P., Tran, L., & Stone, V. (2016). A multi-laboratory toxicological assessment of a panel of 10 engineered NMs to human health-ENPRA project—The highlights, limitations and current and future challenges. *Journal of Toxicology and Environmental Health B Critical Reviews*, *19*, 1–28. https://doi.org/10.1080/10937404.2015.1126210

Kraaijeveld, A. R., Hutcheson, K. A., Limentani, E. C., & Godfray, H. C. J. (2001). Costs of counterdefenses to host resistance in a parasitoid of *drosophila*. *Evolution*, *55*, 1815–1821. https://doi.org/10.1111/j.0014-3820.2001.tb00830.x

Kumar, S., Gautam, C., Mishra, V. K., Chauhan, B. S., Srikrishna, S., Yadav, R. S., … Raj, S. B. (2019). Fabrication of graphene nanoplatelet-incorporated porous hydroxyapatite composites: Improved mechanical and in vivo imaging performances for emerging biomedical applications. *ACS Omega*, *4*, 7448–7458. https://doi.org/10.1021/acsomega.8b03473

Lankoff, A., Arabski, M., Wegierek-Ciuk, A., Kruszewski, M., Lisowska, H., Banasik-Nowak, A., Rozga-Wijas, K., Wojewodzka, M., & Slomkowski, S. (2013). Effect of surface modification of silica nanoparticles on toxicity and cellular uptake by human peripheral blood lymphocytes *in vitro*. *Nanotoxicology*, *7*, 235–250. https://doi.org/10.3109/17435390.2011.649796

Lanot, R., Zachary, D., Holder, F., & Meister, M. (2001). Post-embryonic hematopoiesis in *drosophila*. *Developmental Biology*, *230*, 243–257.

Lasalle, J., & Gauld, I. D. (1991). Parasitic hymenoptera and the biodiversity crisis. *Redia*, *74*, 315–334.

Latouche, M., Lasbleiz, C., Martin, E., Monnier, V., Debeir, T., Mouatt-Prigent, A., Muriel, M. P., Morel, L., Ruberg, M., Brice, A., Stevanin, G., & Tricoire, H. (2007). A conditional pan-neuronal drosophila model of spinocerebellar ataxia 7 with a reversible adult phenotype suitable for identifying modifier genes. *The Journal of Neuroscience*, *27*, 2483–2492. https://doi.org/10.1523/JNEUROSCI.5453-06.2007

Lavine, M. D., & Strand, M. R. (2002). Insect hemocytes and their role in immunity. *Insect Biochemistry and Molecular Biology*, *32*, 1295–1309. https://doi.org/10.1016/S0965-1748(02)00092-9

Leeuw, T. K., Reith, R. M., Simonette, R. A., Harden, M. E., Cherukuri, P., Tsyboulski, D., Beckingham, K. M., & Weisman, R. B. (2007). Single-walled carbon nanotubes in the intact organism: Near-IR imaging and biocompatibility studies in *drosophila*. *Nano Letters*, *7*, 2650–2654. https://doi.org/10.1021/nl0710452

Leitão, A. B., Bian, X., Day, J. P., Pitton, S., Demir, E., & Jiggins, F. M. (2019). Independent effects on cellular and humoral immune responses underlie genotype-by-genotype interactions between *drosophila* and parasitoids. *PLoS Pathogens*, *15*, e1008084. https://doi.org/10.1371/journal.ppat.1008084

Leitão, A. B., & Sucena, É. (2015). *Drosophila* sessile hemocyte clusters are true hematopoietic tissues that regulate larval blood cell differentiation. *eLife*, *4*, e06166. https://doi.org/10.7554/eLife.06166

Lemaitre, B., & Hoffmann, J. (2007). The host defense of *Drosophila melanogaster*. *Annual Review of Immunology*, *25*, 697–743. https://doi.org/10.1146/annurev.immunol.25.022106.141615

Letourneau, M., Lapraz, F., Sharma, A., Vanzo, N., Waltzer, L., & Crozatier, M. (2016). *Drosophila* hematopoiesis under normal conditions and in response to immune stress. *FEBS Letters*, *590*, 4034–4051.

Lindsley, D. L., & Zimm, G. G. (1992). *The genome of Drosophila melanogaster*. Academic Press.

Liu, B., Campo, E. M., & Bossing, T. (2014). *Drosophila* embryos as model to assess cellular and developmental toxicity of multi-walled carbon nanotubes (MWCNT) in living organisms. *PLoS ONE*, *9*, e88681. https://doi.org/10.1371/journal.pone.0088681

Liu, X., Vinson, D., Abt, D., Hurt, R. H., & Rand, D. M. (2009). Differential toxicity of carbon nanomaterials in *drosophila*: Larval dietary uptake is benign, but adult exposure causes locomotor impairment and mortality. *Environmental Science and Technology*, *43*, 6357–6363. https://doi.org/10.1021/es901079z

Lloyd, T. E., & Taylor, J. P. (2010). Flightless flies: *Drosophila* models of neuromuscular disease. *Annuals of the new York Academy of Sciences*, *1184*, E1–E20. https://doi.org/10.1111/j.1749-6632.2010.05432.x

Lux Research. (2014). Nanotechnology update: Corporations up their spending as revenues for nano-enabled products increase. https://portal.luxresearchinc.com/research/report_excerpt/16215

Machado, N. M., Lopes, J. C., Saturnino, R. S., Fagan, E. B., & Nepomuceno, J. C. (2013). Lack of mutagenic effect by multi-walled functionalized carbon nanotubes in the somatic cells of *Drosophila melanogaster*. *Food and Chemical Toxicology*, *62*, 355–360. https://doi.org/10.1016/j.fct.2013.08.051

Martinez, J., Duplouy, A., Woolfit, M., Vavre, F., O'Neill, S. L., & Varaldi, J. (2012). Influence of the virus LbFV and of *Wolbachia* in a host-parasitoid interaction. *PLoS ONE*, *7*(4), e35081. https://doi.org/10.1371/journal.pone.0035081

Maynard, A. D., Aitken, R. J., & Butz, T. (2006). Safe handling of nanotechnology. *Nature*, *444*, 267–269. https://doi.org/10.1038/444267a

McGonigle, J. E., Leitao, A. B., Ommeslag, S., Smith, S., Day, J. P., & Jiggins, F. M. (2017). Parallel and costly changes to cellular immunity underlie the evolution of parasitoid resistance in three *drosophila* species. *PLoS Pathogens*, *13*, e1006683. https://doi.org/10.1371/journal.ppat.1006683

Meyer, D., & Williams, P. L. (2014). Toxicity testing of neurotoxic pesticides in *Caenorhabditis elegans*. *Journal of Toxicology and Environmental Health Part B Critical Reviews*, *17*, 284–306. https://doi.org/10.1080/10937404.2014.933722

Nanogenotox. (2011). http://www.nanogenotox.eu/files/PDF/Deliverables/nanogenotox %20deliverable%203_wp4_%20dispersion%20protocol.pdf.

Nappi, A. J. (1975). Parasite encapsulation in insects. *Invertebrate Immunity*, 293–326. https://doi.org/10.1016/B978-0-12-470265-3.50025-6

Ng, C. T., Yu, L. E., Ong, C. N., Bay, B. H., & Baeg, G. H. (2019). The use of *Drosophila* melanogaster as a model organism to study immune-nanotoxicity. *Nanotoxicology*, *13*, 429–446. https://doi.org/10.1080/17435390.2018.1546413

Pandey, H., Saini, S., Singh, S. P., Gautam, N. K., & Singh, S. (2019). Candle soot derived carbon nanoparticles: An assessment of cellular and progressive toxicity using *Drosophila melanogaster* model. *Comparative Biochemistry and Physiology Part C: Toxicology & Pharmacology*, *228*, 108646.

Pandey, U. B., & Nichols, C. D. (2011). Human disease models in Drosophila melanogaster and the role of the fly in therapeutic drug discovery. *Pharmacological Reviews*, *63*, 411–436. https://doi.org/10.1124/pr.110.003293

Pappus, S. A., & Mishra, M. (2018). A drosophila model to decipher the toxicity of nanoparticles taken through oral routes. *Advances in Experimental Medicine and Biology*, *1048*, 311–322. https://doi.org/10.1007/978-3-319-72041-8_18

Pendleton, R. G., Parvez, F., Sayed, M., & Hillman, R. (2002). Effects of pharmacological agents upon a transgenic model of Parkinson's disease in *Drosophila melanogaster*. *Journal of Pharmacology and Experimental Therapeutics*, *300*, 91–96. https://doi.org/10.1124/jpet.300.1.91

Philbrook, N. A., Walker, V. K., Afrooz, A. R. M. N., Saleh, N. B., & Winn, L. M. (2011). Investigating the effects of functionalized carbon nanotubes on reproduction and development in *Drosophila melanogaster* and CD-1 mice. *Reproductive Toxicology*, *32*, 442–448. https://doi.org/10.1016/j.reprotox.2011.09.002

Priyadarsini, S., Sahoo, S. K., Sahu, S., Mukherjee, S., Hota, G., & Mishra, M. (2019). Oral administration of graphene oxide nano-sheets induces oxidative stress, genotoxicity, and behavioral teratogenicity in *Drosophila melanogaster*. *Environmental Science and Pollution Research*, *26*, 19560–19574. https://doi.org/10.1007/s11356-019-05357-x

Rand, M. D. (2010). Drosophotoxicology: The growing potential for *drosophila* in neurotoxicology. *Neurotoxicology and Teratology*, *32*, 74–83. https://doi.org/10.1016/j.ntt.2009.06.004

Sarkar, B., Mandal, S., Tsang, Y. F., Kumar, P., Kim, K. H., & Ok, Y. S. (2018). Designer carbon nanotubes for contaminant removal in water and wastewater: A critical review. *The Science of the Total Environment*, *612*, 561–581. https://doi.org/10.1016/j.scitotenv.2017.08.132

Sau, T. K., Rogach, A. L., Jackel, F., Klar, T. A., & Feldmann, J. (2010). Properties and applications of colloidal nonspherical noble metal nanoparticles. *Advanced Materials (Deerfield Beach, Fla.)*, *22*, 1805–1825.

Schindelin, J., Arganda-Carreras, I., Frise, E., Kaynig, V., Longair, M., Pietzsch, T., Preibisch, S., Rueden, C., Saalfeld, S., Schmid, B., Tinevez, J. Y., White, D. J., Hartenstein, V., Eliceiri, K., Tomancak, P., & Cardona, A. (2012). Fiji: An open-source platform for biological-image analysis. *Nature Methods*, *9*, 676–682. https://doi.org/10.1038/nmeth.2019

Shen, H., Zhang, L., Liu, M., & Zhang, Z. (2012). Biomedical applications of graphene. *Theranostics*, *2*, 283–294. https://doi.org/10.7150/thno.3642

Siddique, Y. H., Fatima, A., Jyoti, S., Naz, F., Khan, W., Singh, B. R., & Naqvi, A. H. (2013). Evaluation of the toxic potential of graphene copper nanocomposite (GCNC) in the third instar larvae of transgenic *Drosophila melanogaster* (hsp70-lacZ) Bg9. *PLoS ONE*, *8*, e80944. https://doi.org/10.1371/journal.pone.0080944

Siddique, Y. H., Khan, W., Khanam, S., Jyoti, S., Naz, F., Rahul Singh, B. R., & Naqvi, A. H. (2014). Toxic potential of synthesized graphene zinc oxide nanocomposite in the third instar larvae of transgenic *Drosophila melanogaster* (hsp70-lacZ) Bg9. *Biomedical Research International*, *2014*, 382124.

Siegrist, M., Wiek, A., Helland, A., & Kastenholz, H. (2007). Risks and nanotechnology: The public is more concerned than experts and industry. *Nature Nanotechnology*, *2*, 67. https://doi.org/10.1038/nnano.2007.10

Singh, N. P., McCoy, M. T., Tice, R. R., & Schneider, E. L. (1988). A simple technique for quantitation of low levels of DNA damage in individual cells. *Experimental Cell Research*, *175*, 184–191. https://doi.org/10.1016/0014-4827(88)90265-0

Sood, K., Kaur, J., Singh, H., Arya, S. K., & Khatri, M. (2019). Comparative toxicity evaluation of graphene oxide (GO) and zinc oxide (ZnO) nanoparticles on *Drosophila melanogaster*. *Toxicology Reports*, *6*, 768–781. https://doi.org/10.1016/j.toxrep.2019.07.009

Strand, M. R. (2008). The insect cellular immune response. *Insect Sci.*, *15*, 1–14. https://doi.org/10.1111/j.1744-7917.2008.00183.x

Varaldi, J., Petit, S., Boulétreau, M., & Fleury, F. (2006). The virus infecting the parasitoid Leptopilina boulardi exerts a specific action on superparasitism behaviour. *Parasitology*, *132*, 747–756. https://doi.org/10.1017/S0031182006009930

Vecchio, G. (2015). A fruit fly in the nanoworld: Once again *drosophila* contributes to environment and human health. *Nanotoxicology*, *9*, 135–137. https://doi.org/10.3109/17435390.2014.911985

Vega-Alvarez, S., Herrera, A., Rinaldi, C., & Carrero-Martinez, F. A. (2014). Tissue specific direct microtransfer of nanomaterials into *drosophila embryos* as a versatile in vivo test bed for nanomaterial toxicity assessment. *International Journal of Nanomedicine*, *9*, 2031–2041. https://doi.org/10.2147/IJN.S56459

Wang, B., Chen, N., Wei, Y., Li, J., Sun, L., Wu, J., Huang, Q., Liu, C., Fan, C., & Song, H. (2012). Akt signaling-associated metabolic effects of dietary gold nanoparticles in drosophila. *Scientific Reports*, *2*, 563. https://doi.org/10.1038/srep00563 www.lonza.com/qcl1000

Zettervall, C. J., Anderl, I., Williams, M. J., Palmer, R., Kurucz, E., Ando, I., & Hultmark, D. (2004). A directed screen for genes involved in drosophila blood cell activation. *Proceedings of the National Academy of Sciences of the United States of America*, *101*, 14192-141927.

Zhang, W. D., Jiang, L. C., Yu, Y. X., & Wei, X. L. (2014). Electrodeposition of polyaniline onto TiO2 nanoparticles/multiwalled carbon nanotubes for visible light photoelectrocatalysis. *Journal of Nanoscience and Nanotechnology*, *14*, 7032–7037. https://doi.org/10.1166/jnn.2014.8980

Zou, H., Zhao, F., Zhu, W., Yan, L., Chen, H., Gu, Z., Yuan, Q., Zu, M., Li, R., & Liu, H. (2016). *In vivo* toxicity evaluation of graphene oxide in *Drosophila melanogaster* after oral administration. *Journal of Nanoscience and Nanotechnology*, *16*, 7472–7478. https://doi.org/10.1166/jnn.2016.11126

SUPPORTING INFORMATION

Additional supporting information may be found in the online version of the article at the publisher's website.

How to cite this article: Demir, E. (2022). Mechanisms and biological impacts of graphene and multi-walled carbon nanotubes on *Drosophila melanogaster*: Oxidative stress, genotoxic damage, phenotypic variations, locomotor behavior, parasitoid resistance, and cellular immune response. *Journal of Applied Toxicology*, *42*(3), 450–474. https://doi.org/10.1002/jat.4232